Published in final edited form as:

Vet Pathol. 2021 January ; 58(1): 181–204. doi:10.1177/0300985820970144.

Development of mast cell and eosinophil hyperplasia and HLH/MAS-like disease in NSG-SGM3 mice receiving human CD34+ hematopoietic stem cells or patient-derived leukemia xenografts

Laura J. Janke[1], **Denise M. Imai**[2], **Heather Tillman**[1], **Rosalinda Doty**[3], **Mark J. Hoenerhoff**[4,5], **Jiajie J. Xu**[5], **Zach Freeman**[5], **Portia Allen**[5], **Natalie Wall Fowlkes**[6], **Ilaria Iacobucci**[1], **Kirsten Dickerson**[1], **Charles G. Mullighan**[1,7], **Peter Vogel**[1], **Jerold E. Rehg**[1]

[1]Department of Pathology, St. Jude Children's Research Hospital, Memphis, Tennessee, USA

[2]Comparative Pathology Laboratory, University of California, Davis, California, USA

[3]The Jackson Laboratory, Bar Harbor, Maine, USA

[4]In Vivo Animal Core, University of Michigan Medical School, Ann Arbor, Michigan, USA

[5]Unit for Laboratory Animal Medicine, University of Michigan Medical School, Ann Arbor, Michigan, USA

[6]Department of Veterinary Medicine and Surgery, The University of Texas MD Anderson Cancer Center, Houston, Texas, USA

[7]Hematological Malignancies Program, St. Jude Children's Research Hospital, Memphis, Tennessee, USA

Abstract

Immunocompromised mouse strains expressing human transgenes are being increasingly used in biomedical research. The genetic modifications in these mice cause various cellular responses, resulting in histologic features unique to each strain. The NSG-SGM3 mouse strain is similar to the commonly used NSG (NOD *scid* gamma) strain but expresses human transgenes encoding stem cell factor (also known as KIT ligand), granulocyte-macrophage colony-stimulating factor, and interleukin 3. This report describes three histopathologic features seen in these mice when they are unmanipulated or after transplantation with human CD34+ hematopoietic stem cells (HSCs), virally transduced hCD34+ HSCs, or a leukemia patient-derived xenograft. The first feature is mast cell hyperplasia: unmanipulated, naïve mice develop periductular pancreatic aggregates of murine mast cells, whereas mice given the aforementioned human cells develop a proliferative infiltrative interstitial pancreatic mast cell hyperplasia but with human mast cells. The second feature is the predisposition of NSG-SGM3 mice given these human cells to develop eosinophil hyperplasia. The third feature, secondary hemophagocytic lymphohistiocytosis/macrophage activation syndrome (HLH/MAS)–like disease, is the most pronounced in both its

Corresponding author: Laura J. Janke, DVM, PhD, St. Jude Children's Research Hospital, 262 Danny Thomas Place, MS250, Memphis, TN 38105, P:901-595-3165, F:901-595-3100, laura.janke@stjude.org.

Declaration of Conflicting Interests

The authors declare no potential conflicts of interest with respect to the research, authorship, or publication of this article.

clinical and histopathologic presentations. As part of this disease, a small number of mice also have histiocytic infiltration of the brain and spinal cord with subsequent neurologic or vestibular signs. The presence of any of these features can confound accurate histopathologic interpretation; therefore, it is important to recognize them as strain characteristics and to differentiate them from what may be experimentally induced in the model being studied.

Keywords

NSG-SGM3; NSG; hemophagocytic lymphohistiocytosis; macrophage activation syndrome; mast cell hyperplasia; eosinophil hyperplasia

Immunocompromised mice are commonly used in biomedical research, and the various combinations of genetic manipulations have led to an ever-increasing number of different strains being encountered by pathologists.[5,80] One such mouse strain developed specifically to facilitate better engraftment of human myeloid cells and regulatory T cells[11] is the NSG-SGM3 (NOD.Cg-*Prkdc*^{scid} *Il2rg*^{tm1Wjl} Tg(CMV-IL3,CSF2,KITLG)1Eav/MloySzJ) strain (also known as NSGS).[97,98] Because of its immunocompromised status and ability to more readily engraft a variety of human hematopoietic stem and progenitor populations, this strain is used for various immuno-oncology, immunology, and infectious disease studies. The NSG-SGM3 mouse is essentially the NSG (NOD.Cg-*Prkdc*^{scid} *Il2rg*^{tm1Wjl}/SzJ) mouse with the addition of three human transgenes, including those encoding human stem cell factor (SCF, also known as KIT ligand, KITLG), granulocyte-macrophage colony-stimulating factor (GM-CSF, also known as colony stimulating factor 2, CSF2), and interleukin 3 (IL-3). These transgenes were initially expressed in mice on a C57BL/6 × C3H/HeN background, and this line was later backcrossed onto the NSG strain.[67]

The three human cytokine transgenes were chosen for various reasons. Specifically, the SCF/KIT ligand binds to the KIT receptor (CD117)[87] and supports the engraftment and differentiation of myeloid populations. It is also important in mast cell and eosinophil development. It is the only one of the three human cytokines in NSG-SGM3 mice that binds to both mouse and human receptor orthologs.[16] Meanwhile, GM-CSF is another strong inducer of myeloid differentiation,[26] whereas IL-3 can stimulate the proliferation of hematopoietic stem cells (HSCs) and the development of megakaryocytes, in addition to promoting both mast cell and basophil differentiation.[61]

The mice described in this report were either naïve, had been “humanized” by transplantation of human CD34+ HSCs, or had been used to establish models of human leukemia. These mice were humanized by inoculating 4-week-old sublethally irradiated mice with human CD34+ (hCD34+) umbilical cord blood (UCB) HSCs.[62,81] Multilineage hematopoiesis occurs within 12 weeks. Another common use of NSG-SGM3 mice exploits their enhanced ability to engraft different types of human myeloid leukemia,[6,8,97,104] including human leukemia cell lines and leukemia patient-derived xenografts (PDXs). A less common leukemia model involves the implantation of human CD34+ HSCs that have been genetically modified via viral transduction to express leukemia-initiating factors[6,57,95].

This study describes the development of three general categories of histopathologic features in naïve and humanized NSG-SGM3 mice and in NSG-SGM3 mice implanted with transduced hCD34+ HSCs or leukemia PDXs. These features are believed to be due to the expression of the three human transgenes for SCF, GM-CSF, and Il-3 on the NSG background. Briefly, these features are mast cell hyperplasia, eosinophil hyperplasia, and the development of lesions resembling those of secondary hemophagocytic lymphohistiocytosis/macrophage activation syndrome (HLH/MAS). The development of this secondary HLH/MAS-like disease in NSG-SGM3 mice is likely due to activation of macrophages by the three human cytokines, especially GM-CSF. Interestingly, the development of histiocytic proliferations has been previously reported in humanized NSG mice implanted with CD34+ HSCs[42,58,83], and we also include in this paper evidence that these same proliferations develop in NSG mice when implanted with transduced hCD34+ HSCs and leukemia PDXs. The reports in humanized NSG mice did not describe the presence of hemophagocytosis, but it does occur to a mild degree in a subset of humanized NSG mice with histiocytosis[14]. This paper will provide the reader with a comparison of histiocytosis in NSG mice with the more frequently severe hemophagocytic lymphohistiocytosis that develops in NSG-SGM3 mice and provide a rationale for our hypothesis that the NSG strain background of the NSG-SGM3 mice is prone to the proliferation of histiocytes and a mild degree of hemophagocytosis, and that the addition of the transgenes causes exuberant proliferation, activation, and phagocytosis resulting in the clinical syndrome of HLH/MAS-like disease.

In this paper, the features of mast cell and eosinophil hyperplasia and secondary HLH/MAS-like disease are described in NSG-SGM3 and NRG-SGM3 mice associated with studies at four research institutions (St. Jude Children's Research Hospital [St. Jude], the University of California at Davis [UC Davis] via The Jackson Laboratory, the University of Michigan [U Mich], and the University of Texas MD Anderson Cancer Center [MDA]). All the mice associated with these different models exhibited similar phenotypes. One reason that mice from four institutions were evaluated was to examine whether there was an environmental contribution to the observations described. Because we believe the pathology of secondary HLH/MAS-like disease is related to the histiocytosis that can develop in humanized NSG mice, evaluation of the development of histiocytosis in NSG mice having had received transduced hCD34+ HSCs and NSG mice implanted with a B-ALL PDX is included. And finally, because secondary HLH/MAS is known to be associated with infections by viruses and other microorganisms, all NSG-SGM3 mice were examined by *in situ* hybridization (ISH) for the presence of Epstein-Barr virus (EBV), cytomegalovirus (CMV), and *Mycoplasma spp.* to rule out these infections.

Materials and Methods

Mice and experimental models

Animal care at all facilities.—Mice housed at all facilities were maintained under strict specific pathogen free barrier practices using sterilized water, food, bedding, and cages and were handled using aseptic techniques including the use of laminar flow hoods, personal protective equipment and hair coverings. Mice were housed in temperature and humidity controlled rooms that are maintained on a 12:12h light:dark cycle with 10–15

room air changes per hour. All animals had *ad libitum* access to water and food. Mice at all facilities were tested and reported as negative for the following viruses: ectromelia virus, GDVII (Theiler's) virus, lymphocytic choriomeningitis virus (LCMV), mouse adenovirus (MAV), mouse hepatitis virus (MHV), mouse minute virus (MMV), mouse parvovirus (MPV), pneumonia virus of mice (PVM), polyoma virus, reovirus 3, rotavirus (EDIM), and Sendai virus; for the bacterium *Mycobacterium pulmonis*, and for fur mites and pin worms. Mice at St. Jude, The Jackson Laboratory, and MDA were additionally tested and reported as negative for K virus and mouse norovirus (MNV) and the bacteria *Citrobacter rodentium*, *Clostridium piliforme*, *Corynebacterium spp.*, *Filobacterium rodentium* (CAR bacillus), *Helicobacter spp.*, and *Salmonella spp.*. Mice at St. Jude and Jackson Labs were additionally tested and reported as negative for murine chapparvovirus (MuCPV), *Bordetella spp.*, *Streptobacillus moniliformis*, and *Pneumocystis spp*. Mice at The Jackson Laboratory and MDA were additionally tested and reported as negative for Hantaan virus, mouse cytomegalovirus (MCMV), mouse thymic virus (MTV) and *Encephalitozoon cuniculi*. Mice at The Jackson Laboratory were tested and reported as negative for LDH elevating virus (LDEV). Mice at all facilities were on animal use protocols approved by their respective institution's IACUC.

NSG-SGM3 mice.—Evaluation of 3 naïve, unmanipulated mice (one 5-month-old male, one 5-week old male, and one 5-week old female) was performed as part of the routine care and surveillance of a breeding colony of NOD.Cg-*Prkdc*^{scid} *Il2rg*^{tm1Wjl} Tg(CMV-IL3,CSF2,KITLG)1Eav/MloySzJ (NSG-SGM3) mice maintained at St. Jude. This colony was founded in 2014 with stock received from The Jackson Laboratory (Stock No:013062). Every 5 – 10 generations new stock is ordered with a complete turnover of the colony. A total of 25 experimental NSG-SGM3 mice were evaluated for this report and included 14 mice which had been humanized by The Jackson Laboratory, 3 of which were shipped to investigators at the U Mich, 2 to MDA, and 9 remained at the Jackson Laboratory, Sacramento, CA facility. The remaining 11 of the 25 experimental NSG-SGM3 mice were from the St. Jude breeding colony and were associated with leukemia studies conducted at St. Jude. The leukemia models at St. Jude were generated via the implantation of transduced hCD34+ HSCs or a human leukemia PDX (detailed below).

Humanized NSG-SGM3 mice.—Humanization of 14 NSG-SGM3 mice was performed at The Jackson Laboratory when the mice were 4 weeks of age. Mice were irradiated with 100 cGy and injected via tail vein with hCD34+ UCB HSCs. At the respective institutions, mice underwent no other experimental manipulation and were monitored daily. Between 11 and 38 weeks after their arrival animals were submitted for histopathologic evaluation upon exhibiting various clinical signs (Table 1). Mice housed at The Jackson Laboratory were submitted to the Comparative Pathology Laboratory at UC Davis, and the mice at U Mich and MDA were submitted to their respective comparative pathology laboratories.

NSG-SGM3 mice implanted with transduced hCD34+ umbilical cord blood (UCB) HSCs.—Three mice from the St. Jude colony were implanted with human CD34+ UCB cells that had been transduced with a lentiviral vector carrying the fusion gene TCF3-ZNF384, which was predicted to cause leukemia.[25] At 8 weeks of age, 2.5×10^4 GFP-sorted

cells were injected intrafemorally into sublethally irradiated (225 cGy) mice that were monitored daily for signs of illness. Mice were submitted for pathology evaluation between 12 and 20 weeks post-transplant (Table 1).

NSG-SGM3 mice implanted with PDX samples of acute erythroid leukemia (AEL).—The eight NSG-SGM3 mice from AEL PDX studies were also from the St. Jude colony. PDXs were obtained by bone marrow biopsy and stored as cryopreserved cell suspensions in the St. Jude Biorepository. PDX samples were thawed and directly injected into mice without having been cultured or passaged in any mice. Three separate PDX samples were implanted into these eight mice. AEL PDX #1 was implanted into 4 mice, AEL #2 into 3 mice, and AEL#3 into one mouse. At 9 weeks of age, mice were irradiated (250 cGy) prior to transplantation with 1.5 to 2 million cells via tail vein injection. Mice were monitored daily for signs of illness and were submitted for pathology evaluation between 4 and 32 weeks post-transplant.[43] One mouse from each group developed the abnormalities described below and underwent full histopathologic evaluation, and details for these three mice are in Table 1.

NRG-SGM3 mice implanted with AML PDX samples.—Sixteen NRG-SGM3 (NOD.Cg-*Rag1*^{tm1Mom} *Il2rg*^{tm1Wjl} Tg(CMV-IL3,CSF2,KITLG)1Eav/J) mice were obtained by St. Jude from The Jackson Laboratory. These mice differ slightly from the NSG-SGM3 strain in that they have a targeted knockout mutation in the *Rag1* gene instead of in the *Prkdc* gene, but both strains are on the NOD/ShiLtJ genetic background, have a complete null allele of the gene encoding the interleukin 2 receptor common gamma chain, and have transgenic expression of the three human cytokines. This strain shows the same increased ability to engraft myeloid leukemia as does the NSG-SGM3 strain[8]. At 8 weeks of age, mice were irradiated (250 cGy) prior to transplantation with 1.5 million cells via intravenous tail vein injection. All mice received the same AML PDX, which had been collected and stored similarly to the AEL PDXs. Mice were monitored daily for signs of illness and were submitted for pathology evaluation at the experimental endpoint of 20 weeks post-implantation. Those with lesions are detailed in Table 1.

NSG mice.—A total of 23 NSG (NOD.Cg-*Prkdc*^{scid} *Il2rg*^{tm1Wjl}/SzJ) mice from leukemia studies conducted at St. Jude were evaluated. These mice were part of a colony bred at that facility, originally purchased from The Jackson Laboratory (Stock No:005557) and restocked every 5–10 generations. Of these, 5 were implanted with transduced hCD34+ HSCs and 18 with cells of a human B acute lymphoblastic leukemia (B-ALL) PDX.

NSG mice implanted with transduced hCD34+ UCB HSCs.—A group of five mice were implanted as described for NSG-SGM3 mice receiving these cells. At 32 weeks post-implantation all mice were sacrificed with none having shown any clinical signs of illness. Those with lesions are detailed in Table 2.

NSG mice implanted with B-ALL PDX.—A total of 18 mice from a B-ALL study were evaluated. This cohort represented 15 individual PDX samples, with 11 of the 15 samples implanted into one mouse only, 2 of the 15 samples were implanted into 2 mice each, and one of the 15 samples was implanted into 3 mice. PDXs were obtained and treated the

same as the NSG-SGM3 AEL PDX described above. Fourteen of these 18 mice had been irradiated (250 cGy) prior to transplantation via tail vein injection between 8 and 12 weeks of age. Mice were monitored daily and euthanized and submitted for pathology evaluation when they showed clinical signs of illness, between 10 and 38 weeks post-transplant. Those with lesions are detailed in Table 2.

A summary of the number of mice analyzed for each of the above models is shown in Table 3.

Hematology Data

Whole blood was collected from NSG-SGM3 mice nos. 10–20 (Table 1). At all institutions, it was collected via intracardiac puncture while under anesthesia as a terminal procedure. Blood was collected into tubes containing EDTA anticoagulant (BD Microtainer, BD Diagnostics, Franklin Lakes, NJ). Complete blood counts (CBC) at St. Jude were performed on a ForCyte Hematology Analyzer (Oxford Science, Inc, Oxford, CT), at U Mich, on a Hemavet 950FS, and at MDA on an Advia 2120i.

Tissue Processing and Handling

After being euthanized, the tissues collected from each mouse varied. Supplemental Table 1 indicates within each model how many mice had each tissue available for evaluation. The spinal cord was collected from those mice exhibiting ataxia. Organs collected were fixed in 10% neutral-buffered formalin and bones were subsequently decalcified in 10% formic acid. Tissues were embedded in paraffin, sectioned at 4 μm, and stained with hematoxylin and eosin (HE), and unstained slides were used for histochemical stains, immunohistochemistry, and in situ hybridization.

Histochemistry and Immunohistochemistry

The Prussian blue assay for iron was performed on the liver of mice nos. 1–9, 13–21, 25, and 29 as well as on the spleen of mice nos. 1–9, 13–14, 17 25–27, 29 and 30 using an Artisan Iron Stain Kit (Agilent [Dako], Santa Clara, CA, catalog # AR158) in conjunction with an Artisan Link Pro automated slide-staining system (Agilent). Mast cells were identified by using a toluidine blue stain (Poly Scientific, Bay Shore, NY, catalog # S284) and in immunohistochemical (IHC) labeling for mast cell tryptase (MCT) in mice nos. 3, 6, 12–15, and 20 and for c-Kit/CD117 (SCF) in mice nos. 12–14. Cells were identified as human by IHC labeling for human nuclear mitotic apparatus protein (hNuMA1). Cells of eosinophilic lineage were identified by IHC to human-specific and mouse-specific major basic protein (hMBP and mMBP, respectively) in mouse no. 16. In NSG-SGM3 mice, lymphocyte and macrophage cell populations were labeled by IHC for hCD68, hCD163, CD3, hCD4, hCD8, PAX5, hCD45 and F4/80 in the liver of all mice, the spleen of mice nos. 1–17, and the CNS of mice nos. 1–4 and 8–9. Leukemia cells were labeled for GFP in mouse no. 16, GATA1 in mouse no. 20 and myeloperoxidase (MPO) in mice nos. 21–24. In NSG mice, implanted cells were labeled for hCD45 in the spleen of mouse no. 27 and for hNuMA1 in the bone marrow and spleen of mice nos. 25, 26 and 30, and in the liver of mice nos. 27–29. The reactivity for each antibody to the human and mouse antigen was verified by the laboratory

(St. Jude) using either internal or external controls. The sources of antibodies and technical details for IHC assays are provided in Table 4.

In Situ Hybridization

RNAscope ISH probes for *Cytomegalovirus* (catalog #465129) and *Mycoplasma spp.* (catalog #446329) were obtained from Advanced Cell Diagnostics (ACD, Newark, CA), and the assays were performed on a Ventana BenchMark XT automated slide-staining system (Ventana Medical Systems, Tucson, AZ) using the RNAscope VS Duplex Reagent Kit (ACD, catalog #323300). The *Cytomegalovirus* probe was detected using the DISCOVERY mRNA Red HRP Detection Kit (Roche Diagnostics, Indianapolis, IN, catalog #760-234) and the *Mycoplasma spp*. probe was detected using the teal kit (catalog #760-256). EBV was detected by ISH with a probe for EBV-encoded small RNAs (EBER Probe, Leica Biosystems, catalog # PB0589), using the Leica BOND RX automated staining system. A negative control probe for *dapB* and a positive control for *ppiB* were used. External slides from clinical cases at St. Jude known to be positive for each of the organisms were run as positive controls. Assays for each pathogen was performed on the livers of all NSG-SGM3 mice and the spleens of NSG-SGM3 mice 1–17.

Results

Mast cell hyperplasia in NSG-SGM3 mice

Mast cell hyperplasia developed in all NSG-SGM3 mice evaluated by the veterinary pathologists at the institutions included in this study, including all mice described in this report. A murine mast cell hyperplasia occurred in naïve NSG-SGM3 mice which were part of the St. Jude breeding colony, whereas a human mast cell hyperplasia occurred in humanized mice and in mice implanted with transduced hCD34+ cells or a leukemia PDX. Both murine and human mast cell hyperplasia occurred predominantly and to the highest degree in the pancreas, but mild human mast cell hyperplasia also occurred in the stomach, small intestine, lung, spleen, and heart (not shown). Naïve unmanipulated NSG-SGM3 mice presented with varying degrees of periductular pancreatic mast cell accumulation (Fig. 1a). The cells were large and had prominent cytoplasmic granules (Fig. 1a, inset). The nuclei of these cells were not labeled by immunohistochemical staining with hNuMA1, verifying their murine origin (Fig. 1b). Mice implanted with human CD34+ HSCs or a leukemia PDX developed varying degrees of pancreatic infiltrates of human mast cells (Fig. 2a). The human mast cells were smaller than the murine mast cells, had less prominent granules, and spread interstitially instead of forming periductular aggregates (Fig. 2a, inset). Positive nuclear labeling with the antibody to hNuMA1 confirmed their human origin (Fig. 2b). Their identity as mast cells was demonstrated by metachromatic staining of the cytoplasmic granules (Fig. 2c) and by positive immunohistochemical labeling for CD117/c-Kit (Fig. 3a) and mast cell tryptase (MCT) (Fig. 3b). The mice implanted with a leukemia PDX occasionally contained both murine and human mast cells (Figs. 4a and 4b). Human mast cells were also present in much lower numbers in the lamina propria of the stomach and of the small and large intestine, along with occasional resident murine mast cells (not shown).

Eosinophil hyperplasia in NSG-SGM3 mice

The bone marrow of humanized mice, mice implanted with transduced human CD34+ cells, and mice implanted with a leukemia PDX often showed human eosinophil hyperplasia. In humanized mice, the bone marrow eosinophil precursors were in patchy aggregates (Fig. 5 and inset) that varied in number between mice and between bones (sternum, vertebrae, limbs). A similar pattern was seen in mice with transduced-hCD34–derived leukemia (Fig. 6 and inset) and both in AEL and AML leukemia PDXs (Figs. 7 and 8). The eosinophil precursors labeled with hMPB (Fig. 9) and were negative for mMBP (inset).

Histiocytic Proliferation in NSG Mice

Previous reports have documented a histiocytic proliferation in NSG mice when implanted with hCD34+ HSCs,[42,58,83] and the current study found that it can also occur when mice are implanted with transduced hCD34+ HSCs or a B-ALL PDX. Of the five NSG mice implanted with transduced hCD34+ HSCs, two developed large nodules of mature histiocytic cells, including multinucleated giant cells, in the spleen (Fig. 10), bone marrow (Fig. 11), and liver, with one of these 2 showing mild hemophagocytosis and iron accumulation in the splenic red pulp but not in the liver (Table 2). Histiocytic nodules developed in the same tissues in 4 of the 18 mice receiving a B ALL PDX. These four mice were among those which had been irradiated prior to transplantation. The histiocytes in the liver nodules were positive for hNuMA1 (Fig. 12b inset) indicating their human origin. The histiocytes were positive for hCD68 (Fig. 12c) and hCD163 (Fig. 12d) and were surrounded by mouse F4/80-positive macrophages (Fig. 12e). There was no evidence of hemophagocytosis or iron accumulation in two of the four mice (Fig. 12f), while it was present to a mild degree in the other two of the 4 mice (Table 2). The histiocytes were mixed with a few small hCD45+ (Fig. 12g) and CD3+ human lymphocytes (Fig. 12h).

Secondary Hemophagocytic Lymphohistiocytosis/Macrophage Activation Syndrome (HLH/MAS)–Like Disease in NSG-SGM3 mice, General Features

NSG-SGM3 mice developed a secondary HLH/MAS-like disease after undergoing humanization or implantation with transduced hCD34+ HSCs or a leukemia PDX. Morphologically, this disease is somewhat similar to the histiocytosis present in NSG mice, but with a much more activated phenotype as described below. It occurred in approximately 30% of humanized NSG-SGM3 mice (author's observations). The experimental details and clinical signs present in the study mice with this disease are detailed in Table 1. Typical clinical signs included hunched posture, lethargy, and pallor. Unlike in NSG mice with histiocytosis, anemia was a significant component of the HLH/MAS-like disease in NSG-SGM3 mice and was also the most likely cause of clinical illness prompting the removal of mice from a study. Markedly low hematocrit values were common, and the red blood cell parameters indicated a regenerative, macrocytic hypochromic type of anemia. Because a complete blood count (CBC) was not performed for all mice, representative CBC data are shown for three mice: a humanized mouse, a mouse implanted with transduced hCD34+ cells, and a mouse implanted with a leukemia PDX (Table 5). Occasional mice had false indices of hyperchromasia, as shown in Table 5 for the mouse with transduced hCD34+ HSCs.

The histopathologic abnormalities seen in NSG-SGM3 mice with secondary HLH/MAS-like disease are detailed below for each individual model, but many features were common between all. In general, infiltrates of histiocytes with fewer lymphocytes were present predominantly in the spleen and liver, with less frequent and less severe infiltrates in lungs and bone marrow. An important and striking feature of these infiltrates was the marked enlargement of the histiocytes due to accumulation of intracytoplasmic iron and erythrocytes, consistent with hemophagocytosis. The degree of infiltration and organ distribution varied between organs and between the models evaluated as detailed below.

Secondary HLH/MAS-Like Disease in Humanized SGM-SGM3 Mice.—The livers of humanized mice contained sinusoidal, perivascular and portal infiltrates of histiocytes and lymphocytes. The sinusoidal infiltrates were more extensive than the perivascular or portal infiltrates, and occasionally the infiltrates were so severe that they replaced the liver parenchyma and accounted for most of the cells present in the liver (Fig. 13). However, the infiltrates were usually of only moderate severity (Fig. 14a). A large proportion of the inflammatory infiltrates consisted of medium to large macrophages, including multinucleated giant cells of human origin (Fig. 14b and inset), and these cells often contained cytoplasmic Prussian blue positive iron pigment (Fig. 14c). These macrophages expressed hCD68 (Fig. 14d) and hCD163 (Fig. 14e), and the cells were rimmed by mouse macrophages expressing F4/80 (Fig. 14f). The inflammatory infiltrates (Fig. 14g, HE) also consisted of CD3+ T cells (Fig. 14h) and PAX5+ B cells (Fig. 14i), with T cells generally being more numerous than B cells. Most of the T cells were CD4+ cells (Fig. 14j), but low numbers of CD8+ cells were also present (Fig. 14k).

The spleens of humanized mice (Fig. 15a) had a similar composition of cellular infiltrates. The splenic red pulp was variably replaced by nodules or sheets of hNuMA1+ human macrophages (Fig. 15b), some of which had intracellular intact erythrocytes consistent with erythrophagocytosis (Fig. 15c) and many had abundant cytoplasmic iron (Fig. 15d). The splenic macrophages were similar to those in the liver but tended to include more hCD68+ than hCD163+ macrophages (Figs. 15e and 15f, respectively). The splenic white pulp was expanded with human lymphocytes (Fig. 15g) comprising variable proportions of CD3+ T cells (Fig. 15h) and PAX5+ B cells (Fig. 15i). The T cells were a mixture of hCD4+ and hCD8+ cells (Figs. 15j and 15k, respectively), with the former being dominant. Perivascular lymphohistiocytic infiltrates in the lungs were generally of minimal to mild severity and occasionally the histiocytes contained intracytoplasmic iron pigment (Fig. 16). The bone marrow contained variable patchy to scattered infiltrates of large macrophages and multinucleated giant cells (Fig. 17a). These cells occasionally contained intracytoplasmic iron pigment (Fig. 17a, inset), and were positive for hCD68 (Fig. 17b).

Secondary HLH/MAS-Like Disease in Leukemia-Bearing NSG-SGM3 Mice Implanted with Transduced Human CD34+ HSCs.—The mice implanted with transduced human CD34+ HSCs developed a human myelomonocytic leukemia in the liver and bone marrow (Fig. 18a) that consisted of small cells (Fig. 18b) that were positive for myeloperoxidase (MPO) (Fig. 18c) and hCD68 (Fig. 18d). The livers of these mice showed the same histiocyte accumulation with erythrophagocytosis that was seen in the livers of the

humanized mice. Histiocyte aggregates were predominately sinusoidal, with fewer located in portal tracts and around the central veins. They were admixed with moderate numbers of lymphocytes (Fig. 19a). The macrophages often contained cytoplasmic pigment (Fig. 19a) and occasional intact intracytoplasmic erythrocytes (Fig. 19b). Both the macrophages and lymphocytes were of human origin, indicated by positive labeling for hNuMA1 (Fig. 19c). The pigment in the macrophages was identified as iron by Prussian blue staining (Fig.19d). The macrophages were a mixture of hCD68+ and hCD163+ cells (Figs. 19e and 19f, respectively) surrounded by F4/80+ mouse macrophages (Fig. 19g). The transduced leukemia gene had been linked with a GFP reporter, and positively labeled leukemia cell aggregates were apparent (purple chromogen), whereas the large histiocytic cells were negative for GFP (Fig. 19h). These mice had fewer lymphocytes in the liver when compared to the humanized mice, but the lymphocytes that were present were a similar mixture of CD3+ T cells (Fig. 19i) and PAX5+ B cells (Fig. 19j).

The overall cellular composition of the spleen (Fig. 20a) differed from that seen in humanized mice. The white pulp (Fig. 20a, b) was similarly populated by human CD3+ T cells (Fig. 20c) and PAX5+ B cells (Fig. 20d). However, the red pulp (Fig 20a, b) differed significantly from that of the humanized mice in that it was expanded by extramedullary hematopoiesis (EMH) and contained mild to moderate infiltrates of small histiocytes, with a notable absence of large multinucleated giant cells containing cytoplasmic pigment. The small histiocytes differed from those present in the spleens of humanized mice as they were positive for only hCD68 (Fig. 20e) and negative for hCD163 (Fig. 20f).

Secondary HLH/MAS-Like Disease in NSG-SGM3 mice After AEL PDX Implantation.—One mouse per group from each of the three AEL PDX samples developed lesions that were further characterized for the present study. Of these three mice, one had engrafted successfully and two had not. The leukemia PDX that engrafted replaced the bone marrow (Fig. 21a) and was positive for nuclear expression of GATA1[56] (Fig. 21b). Scattered among the leukemia cells in the bone marrow are macrophages containing iron pigment. Surprisingly, the liver had aggregates of human cells (Fig. 22a) that resembled those in humanized mice and in leukemia-bearing mice that had been implanted with transduced human CD34+ cells. The large, multinucleated macrophages had cytoplasmic pigment and occasional intracytoplasmic intact erythrocytes (Fig 22b). The pigment was confirmed to be iron (Fig. 22c). The macrophages were positive for hCD68 and hCD163 (Figs. 22d and 22e, respectively) and were rimmed by F4/80+ mouse macrophages (Fig. 22f). They were admixed with low numbers of GATA1+ leukemia cells (Fig. 22g). Notably, there were no CD3+ T cells (Fig. 22h) nor any PAX5+ B cells present. In the two mice that did not engraft leukemia cells, the liver contained a few macrophage aggregates (Fig. 23a) with cytoplasmic pigment that was positive for iron by Prussian blue staining (Fig. 23b) and occasional CD3+ T cells (Fig. 23c) with no associated PAX5+ B cells. The bone marrow contained low to moderate numbers of macrophages containing iron pigment. Unfortunately, the spleens from these three mice were not available for histopathologic evaluation.

Secondary HLH/MAS-like Disease in NRG-SGM3 mice After AML PDX Implantation.—Sixteen mice from an AML PDX study were evaluated at the experimental

endpoint of 20 weeks. Of these, four exhibited liver histiocytosis with erythrophagocytosis. The leukemia PDX was a myelomonocytic leukemia (Fig. 24) that expressed hCD163, hCD68, and MPO (not shown). However, the liver contained aggregates of cells that did not resemble the leukemia cells but were morphologically macrophages (Fig. 25a) of human origin, as confirmed by positive staining for hNuMA1 (Fig. 25b). The cells showed active erythrophagocytosis (Fig. 25c) and contained cytoplasmic pigment that was positive for iron by Prussian blue staining (Fig. 25d). They were positive for hCD68 and hCD163 (Figs. 25e and 25f, respectively) but only occasional cells expressed MPO (Fig. 25g). These aggregates had no associated CD3+ T cells (Fig. 25h) or PAX5+ B cells.

Central Nervous System Histiocytosis in a Subset of Humanized NSG-SGM3 Mice with HLH/MAS-Like Disease—An interesting phenomenon occurred in a subset of humanized NSG-SGM3 mice with HLH/MAS-like disease that was not seen in the leukemia-bearing mice given transduced hCD34+ HSCs or leukemia PDXs, nor has it been reported in humanized NSG mice to the authors' knowledge. Affected mice developed an accumulation of mixed inflammatory cells in the meninges and an infiltration of macrophages into the central nervous system (CNS) neuropil, predominantly within the cerebellum and regions of the spinal cord. They presented clinically with ataxia, head tilt, and/or hind limb paralysis (Table 1). The cerebellar and spinal cord meninges were thickened (Fig. 26a) with patches of human eosinophils (Fig. 26b), CD3+ T cells (Fig. 26c), and hCD68+ (Fig. 26d) and hCD163+ macrophages. There were also multiple foci of histiocytic cell infiltrates within the neuropil of the spinal cord and cerebellum (Fig. 27a). These cells were large, with abundant cytoplasm; however, in contrast to the cells in the liver and spleen, they had no cytoplasmic pigment and multinucleated giant cells were infrequent (Fig. 27b). The destructive mass effect of the histiocytic infiltrate was sometimes so severe as to suggest a neoplasm, as shown in Figure 27a and highlighted by immunohistochemical staining for hCD68 in Figure 27c. In the areas of neuropil infiltrates, only small numbers of lymphocytes were present along the border of the sheets of macrophages (Fig. 27d). Mouse F4/80-positive macrophages were also increased along the border (Fig. 27e).

Evaluation for EBV, CMV, and Mycoplasma

Because the presence of infectious agents is associated with the development of secondary HLH/MAS, all samples were analyzed for the presence of three pathogens by ISH. All of the tested samples (detailed in methods) were determined to be negative.

Discussion

A summary of the histopathologic features of the NSG-SGM3 mice described in this report and a comparison with what is observed in NSG mice are provided in Table 6. All of the lesions observed in the NSG-SGM3 mice in this study developed because human cells with the ability to differentiate into mast cells, eosinophils, and macrophages were implanted into the mice. For the humanized mice, this source was the implanted hCD34+ HSCs. In the case of the leukemia model created by injecting transduced hCD34+ HSCs, the source of cells comprising the lesions was probably non-transduced hCD34+ HSCs that were implanted along with the transduced leukemia progenitor cells. This is supported

by the fact that the large human macrophages in the liver were negative for the GFP reporter. The non-transduced cells were likely a very small contaminating population as the cells had been GFP-sorted prior to implantation. The cell of origin in the leukemia PDX models is presumably a stem/progenitor population introduced with the PDX leukemia cells. This theory is supported by the observation of one of the authors (L.J.J., unpublished data) that these lesions do not occur in NSG-SGM3 mice implanted with leukemia cell lines, suggesting that there is a contributing population within the PDX other than the neoplastic cells. The complex cellular environment of a PDX has both positive and negative consequences. PDX models are often employed when one is unable to develop a tumor cell line from a patient-derived sample, in which case the leukemia is established in immunocompromised mice. It is assumed that the additional cell types that are present provide supportive factors that enable PDX samples to proliferate in mice, and this cellular heterogeneity is one of the features that makes them more attractive than using tumor cell lines.[21,82,96] PDXs contain numerous cell types in addition to neoplastic cells, including stromal cells, blood vessel cells, immune cells, and importantly, hematopoietic progenitors. However, these additional cellular factors might contribute to the negative consequences sometimes seen as a result of PDX implantation, and likely to the development of the secondary HLH/MAS-like disease described in this paper. Other negative consequences have been demonstrated in the numerous reports of post-transplant lymphoproliferative disorders (PTLD) in NSG mice implanted with solid tumors[20,31,69,88,103] and of post-transplant graft-versus-host disease (GvHD).[77] PTLD generally involves the development of multisystemic lymphoplasmacytic infiltrates containing predominantly T cells with fewer B cells and/or B cell lymphoma.[50,64,88] GvHD is characterized largely by T cell infiltrates with damage to the epithelia of the skin, lung, liver, and gastrointestinal tract.[29,33] The inflammatory cell infiltrates in both PTLD and GvHD are of human origin and are believed to be derived from the xenograft. Notably, no abnormalities were present in the skin and gastrointestinal tract of the NSG-SGM3 mice in this study, and the lesions present in the lungs and liver did not include damage to epithelia. Furthermore, an important distinction between PTLD and GvHD and the inflammatory cell proliferations reported here in NSG-SGM3 mice is the predominance of myeloid-derived cellular proliferations (mast cells, eosinophils, and macrophages) in NSG-SGM3 mice. The following discussion will separately address the 3 categories of immune cell proliferations described in this report.

Mastocytosis

Given that SCF and IL-3 are important in mast cell development, it is not entirely unexpected that NSG-SGM3 mice can develop mast cell hyperplasia. The proliferation of mouse mast cells is the only abnormality regularly observed in naïve NSG-SGM3 mice, and it occurs because human SCF is cross-reactive and is, therefore, able to bind and activate murine SCF receptors.[16] The role of SCF in myeloid cell engraftment was studied by creating a mouse expressing membrane-bound human SCF (hSCF) on an NSG background.[87] After being humanized, these hSCF-NSG mice showed increased numbers of human mast cells when compared to humanized NSG mice without the transgenic hSCF, suggesting that this cytokine is sufficient for the proliferation of human mast cells. Unlike the situation in mice, in which recombinant murine IL-3 has been shown to be a strong inducer of mast cell proliferation,[63] human IL-3 does not by itself induce mast cell

proliferation[51] but must be combined with other cytokines such as SCF[52] and/or interleukin 6 (IL-6)[76] to induce optimal mast cell proliferation. Previous studies using the NSG-SGM3 mouse have reported the presence of increased mast cells in various tissues such as the lung, spleen, stomach, small intestine, heart, and skin.[6,17] We similarly observed low numbers of human mast cells in all of these tissues except the skin. In the skin we observed moderate numbers of mast cells positive for MCT, but these were negative for hNuMA1, indicating that they were murine mast cells. The reason for the discrepancy between our findings and others is not clear but may be due to the antibody used to detect MCT. Although the antibody we used is labeled for human MCT, we observed in our own testing that it also labels mouse mast cells. Therefore, it is possible that the cells labeled in these previous publications were murine, as they were not verified to be human via hNuMA1 positivity or other such human-specific antigens. This is the first report of the presence of high numbers of human mast cells in the pancreas. It is possible that they were present in the mice examined in previous studies[6,17] but this specific tissue was not examined. It is unclear why the pancreas is a target organ for mast cells in these mice, as no clear role has yet been described for mast cells in either pancreatic homeostasis or pancreatic disease.

Eosinophil hyperplasia

Eosinophil development and differentiation are dependent on essentially 3 cytokines: IL-3, GM-CSF, and interleukin 5 (IL-5).[32] In NSG-SGM3 mice, the excess production of both IL-3 and GM-CSF probably drives implanted HSCs toward eosinophil differentiation and hyperplasia. IL-3 and GM-CSF are necessary to promote the expansion of immature cells, which then commit to eosinophil/basophil differentiation upon the binding of IL-5.[32] Thus, the development of eosinophil hyperplasia in the NSG-SGM3 mouse is dependent upon the addition of IL-5. This could be provided by the implanted human cells or by the mouse itself, as murine and human IL-5 are cross-reactive.[59] The main source of IL-5 is CD4+/T_H2 cells;[61] in humanized mice the IL-5 may be provided by the numerous engrafted human CD4+ T cells evident in the spleen and liver in the present study.

Secondary HLH/MAS-Like Disease

We have described the complex phenotype of the multisystemic accumulation of human macrophages, often accompanied by human lymphocytes, and the associated hemophagocytosis that occurs predominantly in the spleen and liver of NSG-SGM3 mice. This lesion occurred in a subset of humanized mice with no additional experimental manipulation between 11 and 38 weeks post humanization. A similar phenotype resulted when NSG-SGM3 mice were implanted with transduced hCD34+ HSCs or a leukemia PDX. The hemophagocytosis resulted in profound anemia, lethargy, overall poor health, and eventual morbidity requiring euthanasia. The macrophages were positive for hCD68 and hCD163, suggesting that these were more differentiated cells rather than immature macrophages[27], with a tendency toward the M2 macrophage phenotype.[65] The macrophages had large accumulations of iron, and frank erythrophagocytosis was visible. These histopathologic findings, along with CBC data indicating a hemolytic anemia, suggest the mice have secondary HLH/MAS-like disease.

Our data enable a comparison between the appearance of histiocytic proliferation with occasional mild hemophagocytosis in NSG mice that have been humanized[42,58,83] or implanted with a PDX and the appearance and clinical manifestations of secondary HLH/MAS in similarly treated NSG-SGM3 mice. When describing histiocyte proliferations in humanized NSG mice that were not reported to be associated with hemophagocytosis, Huey et al. used the diagnostic terms granulomatous inflammation and granulomatosis. Given the proliferation of large epithelioid macrophages with multinucleated giant cells, this diagnosis is reasonable. In the current paper, we have chosen to use the term histiocytosis because of the suspected connection with secondary HLH/MAS-like disease in NSG-SGM3 mice. It appears that the NSG strain background of the NSG-SGM3 mice is prone to the proliferation of histiocytes that sometimes exhibit hemophagocytosis, and the addition of the SGM3 transgenes (specifically GM-CSF as detailed below) causes exuberant proliferation, activation, and phagocytosis resulting in the clinical syndrome of HLH/MAS-like disease. Differentiating a hemophagocytic histiocytosis (such as that shown here in NSG-SGM3 mice) from other types of histiocytic proliferations (as shown in some NSG mice) is important both in animal models and in human diagnostics because other histiocytic disorders can show occasional hemophagocytosis cytologically and histologically.[72] Unfortunately there is no consensus on criteria for pathological hemophagocytosis vs. occasional, incidental hemophagocytosis.[36,70] Key factors in establishing the diagnosis of a hemophagocytic disorder include the clinical appearance of anemia with or without other cytopenias, along with a high number of hemophagocytes. In humans, associated laboratory data are considered to be essential to making this diagnosis.[48] In the case of the NSG-SGM3 mice described in this paper, the clinical features and very high number of hemophagocytes suggest they have true pathological hemophagocytosis. This delineation in the subset of NSG mice that show hemophagocytosis is less clear. In the three NSG mice implanted with transduced hCD34+ HSCs or a B-ALL PDX that had iron accumulation in the histiocytes, none had clinical signs suggesting anemia, but unfortunately blood for CBCs was not collected.

HLH/MAS is a syndrome of pathologic immune activation.[48] It is believed to result from lymphocytes activating macrophages, leading to excessive cytokine production and eventually a cytokine storm. In humans, HLH is characterized by fever, splenomegaly, cytopenias, increased triglycerides/decreased fibrinogen, and hemophagocytosis.[40] There are two types of HLH: genetic or familial (F-HLH) and secondary, of which the latter encompasses several subtypes. F-HLH was first described in 1952.[28] The first underlying genetic defect—mutations in the *PRF1* gene encoding perforin—was discovered in 1999.[85] Secondary HLH can be incited by numerous conditions, including many different types of infection, with EBV, CMV, and HIV being the most common viral causes.[70,75] Secondary HLH can also be associated with rheumatologic disorders and is commonly referred to as macrophage activation syndrome (MAS) in the setting of rheumatologic disease. It is also associated with malignancy, immune compromise, and immune-activating therapies[48]. Relevant to the development of HLH/MAS-like disease in NSG-SGM3 mice described in this paper, both hematologic transplant and solid organ transplant are associated with HLH/MAS in humans, and it is more frequent in patients receiving UCB than in those receiving autologous or allogenic transplants.[1,3] Diagnosis is difficult and relies on a

specific set of criteria based on clinical signs, hematology, and clinical chemistry findings.[48] Five of these eight criteria must be fulfilled for diagnosis: fever >38.3° C; splenomegaly; cytopenias; hypertriglyceridemia; hemophagocytosis in bone marrow, spleen, lymph nodes, or liver; low or absent NK-cell activity; ferritin >500 ng/mL, and elevated soluble CD25.[48] In the HLH/MAS-like disease present in NSG-SGM3 mice, we did not evaluate for fever, hypertriglyceridemia, NK-cell activity, ferritin, and soluble CD25. However, some of the criteria for diagnosis in humans were fulfilled in these mice, including splenomegaly, cytopenias, and hemophagocytosis. What is known regarding the histopathology present in humans with HLH/MAS comes predominantly from bone marrow and liver biopsies. The bone marrow contains increased macrophages with a proportion of them demonstrating hemophagocytosis, although the sole finding of hemophagocytosis in bone marrow biopsies is neither sensitive nor specific for HLH/MAS.[36,70] The livers of these patients show sinusoidal dilatation with proliferation of activated macrophages with hemophagocytosis and cytoplasmic pigment/iron.[24] Portal inflammation consists of variably sized lymphocytes with few histiocytes. The macrophages in the bone marrow and liver can be identified by immunohistochemical labeling for CD68[12] or CD163.[7,71]

A key factor in HLH/MAS is that it is the exaggerated immune response, culminating in a cytokine storm, that drives the disease pathology, not the underlying primary infection or another associated disorder. This dysregulated immune activation differs from many other immune disorders in that self-reactivity/autoimmunity is not the underlying mechanism.[48] Most of our current understanding of the pathophysiology of HLH is based on genetic animal models with defects in the *PRF1* gene. The results of these studies have suggested that although macrophages have a role in disease development, it is T cells (specifically CD8+ T cells) that are the key upstream drivers of HLH disease.[68] Interferon gamma (IFN-γ) has also been demonstrated to be a key mediator of disease development and is most likely the main coupler between activated T cells and activation of macrophages.[105] These findings highlight a key difference in the HLH-like disease in NSG-SGM3 mice described in this paper: although there were T cells present, there were far more CD4+ T cells than CD8+ T cells, which is inconsistent with the findings in genetic models of this disease. This suggests that the genetic model of F-HLH, which primarily uses perforin-deficient mice, does not completely mimic what occurs in the numerous forms of secondary HLH/MAS.

What is common to F-HLH and secondary HLH is that macrophages are central to disease development, and it is their activation and subsequent cytokine production that is key. However, in secondary HLH, CD8+ T cells may be sufficient upstream drivers of macrophage activation, although not necessary. The ability of macrophages by themselves to mediate the development of secondary HLH has been suggested by studies in which repeated TLR9[10] stimulation produced an HLH/MAS-like disease in mice; this was found to be dependent on IFN-γ but not on the presence of lymphocytes.[19] Recently, Akilesh and colleagues described the ability of chronic TLR7 and TLR9 signaling to stimulate the development of a type of macrophage they termed an “inflammatory hemophagocyte,”[4] suggesting a link between TLR signaling and the activation of macrophages leading to HLH/MAS-like disease.

The primary role of macrophages and the lesser role of lymphocytes in HLH/MAS pathogenesis has been demonstrated in several mouse studies.[15,99,100] The authors of one such study injected NSG-SGM3 mice with unfractionated UCB that had been depleted of T cells, which induced a syndrome that the authors identified as MAS and that resembled the secondary HLH/MAS-like disease described in the present study.[99] Of the mice so treated, 30% became moribund between 16 and 20 weeks of age, which is similar to the latency observed in the present study. Anemic, clinically ill mice treated with dexamethasone, immunoglobulin, or anti-B/T cell antibodies showed no improvement, whereas treatment with gemtuzumab ozogamicin, a CD33-targeting myeloablating drug, resulted in the reversal of anemia and a marked improvement in their clinical appearance. An analysis of serum cytokines from the UCB-engrafted mice showed a significant increase in IL-6 and small but insignificant increases in IFNγ and tumor necrosis factor α (TNFα), which have been demonstrated to be key drivers in genetic models of HLH.[46,54,105] A separate study followed the development of post-transplant HLH in NSG-SGM3 mice humanized by a different method using hCD34+ fetal liver cells.[100] In that study, there was a similar latency period of 17 to 22 weeks, and histologic liver lesions resembled those described in the present report, with an accumulation of large multinucleated hCD68+ macrophages containing iron, and CD3+ T cells. Flow cytometry analysis of peripheral blood T-cell subsets showed an increased CD4:CD8 ratio, which is consistent with the findings in the present study. The serum levels of numerous cytokines, namely IFNγ, TNFα, IL-6, and GM-CSF, were elevated in the humanized NSG-SGM3 mice, as compared to the non-humanized NSG-SGM3 mice.[100] The finding of increased IL-6 in these two studies is consistent with what has been found in some human HLH/MAS studies.[22,71] However, IL-6 inhibition with tocilizumab (an anti-IL6R antibody) has not proved effective at treating the disease in humans.[35,78]

Regarding the disease in NSG-SGM3 mice described in this report, overexpressed human GM-CSF is probably the key macrophage-activating cytokine driving secondary HLH/MAS-like disease. Briefly, this is because human studies and animal models of HLH/MAS have shown it to be a key cytokine in driving the disease, and because GM-CSF is a known potent activator of macrophages. This cytokine can act directly upon the implanted cells because the receptor for GM-CSF is expressed on human CD34+ hematopoietic progenitors.[79] GM-CSF is not essential for normal homeostasis, but it participates in the rapid expansion and differentiation of myeloid cells as part of an inflammatory response.[26] The exact function of GM-CSF in various disease conditions is complex, as it has been implicated in promoting numerous inflammatory diseases such as rheumatoid arthritis, multiple sclerosis, and some forms of colitis, whereas other studies have shown it to promote anti-tumor immunity and to participate in the resolution of inflammation during infection.[9,26,102] An extensive body of research has demonstrated the myriad roles of GM-CSF in hematopoiesis and inflammation. Relevant to the current study is the demonstration that GM-CSF induced HLH in a human patient receiving the cytokine along with chemotherapy for lymphoma.[73] Similarly, it was shown to exacerbate hemophagocytosis associated with myelodysplastic syndrome.[94] Reviews of GM-CSF are available.[9,26,38,90,102] Here we will discuss only selected studies that are directly relevant to the contribution of GM-CSF to the development of the HLH/MAS-like disease in NSG-SGM3 mice.

The most relevant role of GM-CSF in relation to the development of the secondary HLH/MAS-like disease in NSG-SGM3 mice is its effect on macrophages. *In vitro* studies have shown that when grown in culture in the presence of GM-CSF, mouse bone marrow will produce both macrophages ($MHCII^{low}F4/80^{high}$) and dendritic cells ($MHCII^{high}F4/80^{low}$) but that the proportion of macrophages increases with increasing doses of GM-CSF.[66] The types of macrophages that develop under the influence of GM-CSF are not clearly of the M1 or M2 type.[65] They produce higher levels of inflammatory cytokines, specifically TNF-α, IL-6, interleukin 12 p70 (IL-12p70), and interleukin 23 (IL-23), than do M-CSF (macrophage colony-stimulating factor)–derived macrophages[30] or GM-CSF–derived dendritic cells.[66] The transgenic expression of GM-CSF in NSG-SGM3 mice could well be at a sufficiently high level to drive the production of large numbers of macrophages expressing high amounts of inflammatory cytokines, thereby influencing the development of secondary HLH/MAS-like disease.

The *in vivo* role of GM-CSF has been investigated by inducing its overexpression in mice.[55] The most remarkable hematopoietic finding was the marked accumulation of peritoneal macrophages that were twice the size of the controls. Interestingly, these cells had enhanced Fc-dependent phagocytosis of antibody-coated sheep erythrocytes,[89] perhaps providing evidence that GM-CSF drives hemophagocytosis in secondary HLH/MAS-like disease. This model also showed prominent infiltration of macrophages into the eyes, primarily in the vitreous humor but also in the anterior and posterior chambers and subretinally.[55] Such eye lesions were not present in the mice examined in the present study.

Further research has examined the effects of the production of GM-CSF by specific cell types. When examined at 6 weeks of age, C57BL/6 mice with conditional overexpression of GM-CSF in their T cells showed partial effacement of the lymph nodes, spleen, and thymus by histiocyte-like cells, with occasional multinucleated giant cells.[92] The lung, kidney, and liver had varying degrees of granulocyte and histiocyte infiltration. Evaluation of the histiocyte-like cells by flow cytometry revealed them to be a mixture of monocytes, macrophages, and dendritic cells.

In the present study we found a proliferation of histiocytes in the CNS of some humanized NSG-SGM3 mice, which we have not seen, nor are we aware of being reported, in humanized NSG mice. Although we did not observe hemophagocytosis within these CNS lesions in the mice, CNS involvement does occur with HLH/MAS in humans. It is generally estimated that around one third of patients with HLH/MAS show CNS symptoms[41,45,48] but some studies have observed as high as 73%.[37] Diagnosis is generally made using MRI or CT imaging.[18,34] Occasionally a brain biopsy is undertaken or the diagnosis is made at autopsy. Lesions in the brain range from mild histiocytic or lymphohistiocytic leptomeningeal infiltrates to diffuse infiltration of the neuropil with large numbers of CD68+ histiocytes and CD3+ T cells with fewer B cells.[39,49,53]

We suspect that the activity of GM-CSF is implicated in the nervous system abnormalities. Interestingly, conditional expression of GM-CSF in the peripheral CD4+ T cells of C57BL/6 mice[84] resulted in neurologic defects (ataxia, circling) around 12 weeks after induction. Early in the process, this was associated with CNS-infiltrating myeloid cells (monocytes and

neutrophils) but with a notable absence of T cells, whereas later in the disease course, T cells began to infiltrate as well. These cells often formed solid masses, particularly in the brain stem and, less abundantly, in the spinal cord, which was the same pattern observed in the mice in the present study. RNA sequencing showed the gene expression profile of inflammatory monocyte-derived cells in the CNS to be vastly different from that of similar cells in all other organs examined.[84] Further characterization of the histiocytic subsets that are composing these lesions in the NSG-SGM3 mice is needed to see if they represent a unique population.

An interesting question yet to be answered is why only some mice develop secondary HLH/MAS-like disease, and why a subset of those then go on to develop the CNS phenotype. Their development may be influenced by host factors and/or factors intrinsic to the implanted cells. We theorized that some hCD34+ HSCs and PDXs contain inactive microorganisms which are reactivated following introduction into the immunocompromised NSG-SGM3 mouse. The lesions were examined for the presence of EBV and CMV because of their association with HLH/MAS[70,75], and for mycoplasma because of its propensity to contaminate cell products and affect experimental findings.[13,91,101] By ISH, these organisms were not detected in our samples, which suggests they are not the cause in this group of mice. Additional studies are necessary to determine the initiating factors, with the goal being to eliminate these factors and thus prevent the development of this confounding syndrome.

The results of our study indicate that when evaluating NSG-SGM3 mice that have been implanted with human cells, one must carefully confirm the cell population(s) generated. We demonstrated how this is important in the context of leukemia studies, but it is also relevant in other study types such as infectious disease studies. The complexity of cell populations is compounded in studies combining multiple types of implanted human cells, as is often done for immunotherapy.[21,23,86] Such studies have been conducted in NSG mice, including the use of anti-PD1[74,93] and CAR-T[2,47] cell therapy. These studies have shown humanized mice to be a superior model in testing immunotherapies, and it is likely that similar studies in NSG-SGM3 mice are currently being conducted. All three of the features described here could confound the results of studies using NSG-SGM3 mice. Because the proliferating human mast cells do not resemble typical mouse connective tissue mast cells, they may be mistaken for other cell types. Although eosinophils are not difficult to recognize in tissue sections, one might misinterpret their increased number as being completely due to the experimental manipulation instead of recognizing that the human transgenes could be affecting their numbers. Regarding the occurrence of secondary HLH/MAS-like disease, the use of survival or CBC data such as anemia as an endpoint must be accompanied by histopathologic evaluation in order to confirm the cause of death. This is particularly important in AML studies, in which anemia leading to lethargy and eventual euthanasia is a commonly used endpoint,[44,60] as the causes of the anemia could be confusing and difficult to differentiate.

It is possible that future studies will demonstrate that the disease seen in NSG-SGM3 mice, which we have termed secondary HLH/MAS-like disease, does in fact reflect the condition in humans and may serve as a model of HLH/MAS. As so many conditions are associated with the development of the syndrome in humans, the final manifestations are

probably an endpoint associated with numerous pathways. In view of this, it is likely that no single model will be able to mimic the human condition completely, but perhaps the lesions described here will provide some insight into its mechanisms.

Supplementary Material

Refer to Web version on PubMed Central for supplementary material.

Acknowledgements

The authors thank the St. Jude Animal Resource Center and the Veterinary Pathology Core for technical assistance. The authors thank Keith A. Laycock, PhD, ELS, for scientific editing of the manuscript.

Funding

This publication was supported, in part, by grants R35CA197695-01A1 and CA021765 from the National Cancer Institute, The St Jude Chromatin Collaborative, The Leukemia and Lymphoma Society Translational Research Program, and the American Lebanese Syrian Associated Charities (ALSAC). The content is solely the responsibility of the authors and does not necessarily represent the official views of the National Institutes of Health.

References

1. Abdelkefi A, Jamil WB, Torjman L, Ladeb S, Ksouri H, Lakhal A, et al.: Hemophagocytic syndrome after hematopoietic stem cell transplantation: a prospective observational study. Int J Hematol2009:89(3):368–373. [PubMed: 19252966]
2. Agarwal S, Hanauer JDS, Frank AM, Riechert V, Thalheimer FB, Buchholz CJ: In Vivo Generation of CAR T Cells Selectively in Human CD4(+) Lymphocytes. Mol Ther2020:28(8):1783–1794. [PubMed: 32485137]
3. Akamatsu N, Sugawara Y, Tamura S, Matsui Y, Hasegawa K, Imamura H, et al.: Hemophagocytic syndrome after adult-to-adult living donor liver transplantation. Transplant Proc2006:38(5):1425–1428. [PubMed: 16797322]
4. Akilesh HM, Buechler MB, Duggan JM, Hahn WO, Matta B, Sun X, et al.: Chronic TLR7 and TLR9 signaling drives anemia via differentiation of specialized hemophagocytes. Science2019:363(6423).
5. Allen TM, Brehm MA, Bridges S, Ferguson S, Kumar P, Mirochnitchenko O, et al.: Humanized immune system mouse models: progress, challenges and opportunities. Nat Immunol2019:20(7):770–774. [PubMed: 31160798]
6. Askmyr M, von Palffy S, Hansen N, Landberg N, Hogberg C, Rissler M, et al.: Transgenic expression of human cytokines in immunodeficient mice does not facilitate myeloid expansion of BCR-ABL1 transduced human cord blood cells. PLoS One2017:12(10):e0186035. [PubMed: 29023488]
7. Avcin T, Tse SM, Schneider R, Ngan B, Silverman ED: Macrophage activation syndrome as the presenting manifestation of rheumatic diseases in childhood. J Pediatr2006:148(5):683–686. [PubMed: 16737887]
8. Barve A, Casson L, Krem M, Wunderlich M, Mulloy JC, Beverly LJ: Comparative utility of NRG and NRGS mice for the study of normal hematopoiesis, leukemogenesis, and therapeutic response. Exp Hematol2018:67:18–31. [PubMed: 30125602]
9. Becher B, Tugues S, Greter M: GM-CSF: From Growth Factor to Central Mediator of Tissue Inflammation. Immunity2016:45(5):963–973. [PubMed: 27851925]
10. Behrens EM, Canna SW, Slade K, Rao S, Kreiger PA, Paessler M, et al.: Repeated TLR9 stimulation results in macrophage activation syndrome-like disease in mice. J Clin Invest2011:121(6):2264–2277. [PubMed: 21576823]
11. Billerbeck E, Barry WT, Mu K, Dorner M, Rice CM, Ploss A: Development of human CD4+FoxP3+ regulatory T cells in human stem cell factor-, granulocyte-macrophage colony-

stimulating factor-, and interleukin-3-expressing NOD-SCID IL2Rgamma(null) humanized mice. Blood2011:117(11):3076–3086. [PubMed: 21252091]

12. Billiau AD, Roskams T, Van Damme-Lombaerts R, Matthys P, Wouters C: Macrophage activation syndrome: characteristic findings on liver biopsy illustrating the key role of activated, IFN-gamma-producing lymphocytes and IL-6- and TNF-alpha-producing macrophages. Blood2005:105(4):1648–1651. [PubMed: 15466922]
13. Birke C, Peter HH, Langenberg U, Muller-Hermes WJ, Peters JH, Heitmann J, et al.: Mycoplasma contamination in human tumor cell lines: effect on interferon induction and susceptibility to natural killing. J Immunol1981:127(1):94–98. [PubMed: 7195412]
14. Blümich S, Zdimerova H, Münz C, Kipar A, Pellegrini G: Human CD34(+) Hematopoietic Stem Cell-Engrafted NSG Mice: Morphological and Immunophenotypic Features. Vet Pathol2020:300985820948822.
15. Brisse E, Imbrechts M, Mitera T, Vandenhaute J, Wouters CH, Snoeck R, et al.: Lytic viral replication and immunopathology in a cytomegalovirus-induced mouse model of secondary hemophagocytic lymphohistiocytosis. Virol J2017:14(1):240. [PubMed: 29258535]
16. Broxmeyer HE, Cooper S, Lu L, Hangoc G, Anderson D, Cosman D, et al.: Effect of murine mast cell growth factor (c-kit proto-oncogene ligand) on colony formation by human marrow hematopoietic progenitor cells. Blood1991:77(10):2142–2149. [PubMed: 1709371]
17. Bryce PJ, Falahati R, Kenney LL, Leung J, Bebbington C, Tomasevic N, et al.: Humanized mouse model of mast cell-mediated passive cutaneous anaphylaxis and passive systemic anaphylaxis. J Allergy Clin Immunol2016:138(3):769–779. [PubMed: 27139822]
18. Cai G, Wang Y, Liu X, Han Y, Wang Z: Central nervous system involvement in adults with haemophagocytic lymphohistiocytosis: a single-center study. Ann Hematol2017:96(8):1279–1285. [PubMed: 28589450]
19. Canna SW, Wrobel J, Chu N, Kreiger PA, Paessler M, Behrens EM: Interferon-gamma mediates anemia but is dispensable for fulminant toll-like receptor 9-induced macrophage activation syndrome and hemophagocytosis in mice. Arthritis Rheum2013:65(7):1764–1775. [PubMed: 23553372]
20. Chen K, Ahmed S, Adeyi O, Dick JE, Ghanekar A: Human solid tumor xenografts in immunodeficient mice are vulnerable to lymphomagenesis associated with Epstein-Barr virus. PLoS One2012:7(6):e39294. [PubMed: 22723990]
21. Choi Y, Lee S, Kim K, Kim SH, Chung YJ, Lee C: Studying cancer immunotherapy using patient-derived xenografts (PDXs) in humanized mice. Exp Mol Med2018:50(8):99.
22. Crayne CB, Albeituni S, Nichols KE, Cron RQ: The Immunology of Macrophage Activation Syndrome. Front Immunol2019:10:119. [PubMed: 30774631]
23. Curran M, Mairesse M, Matas-Cespedes A, Bareham B, Pellegrini G, Liaunardy A, et al.: Recent Advancements and Applications of Human Immune System Mice in Preclinical Immuno-Oncology. Toxicol Pathol2020:48(2):302–316. [PubMed: 31847725]
24. de Kerguenec C, Hillaire S, Molinie V, Gardin C, Degott C, Erlinger S, et al.: Hepatic manifestations of hemophagocytic syndrome: a study of 30 cases. Am J Gastroenterol2001:96(3):852–857. [PubMed: 11280564]
25. Dickerson K, Yoshihara H, Janke L, Mullighan CG: Expression of TCF3-ZNF384 in Human Hematopoietic Cells Induces Lineage Disruption in Vitro and Acute Leukemia in Vivo. Blood2018:132(Supplement 1):550–550.
26. Dougan M, Dranoff G, Dougan SK: GM-CSF, IL-3, and IL-5 Family of Cytokines: Regulators of Inflammation. Immunity2019:50(4):796–811. [PubMed: 30995500]
27. Fabriek BO, Dijkstra CD, van den Berg TK: The macrophage scavenger receptor CD163. Immunobiology2005:210(2–4):153–160. [PubMed: 16164022]
28. Farquhar JW, Claireaux AE: Familial haemophagocytic reticulosis. Arch Dis Child1952:27(136):519–525. [PubMed: 13008468]
29. Ferrara JL, Levine JE, Reddy P, Holler E: Graft-versus-host disease. Lancet2009:373(9674):1550–1561. [PubMed: 19282026]
30. Fleetwood AJ, Lawrence T, Hamilton JA, Cook AD: Granulocyte-macrophage colony-stimulating factor (CSF) and macrophage CSF-dependent macrophage phenotypes display differences

in cytokine profiles and transcription factor activities: implications for CSF blockade in inflammation. J Immunol2007:178(8):5245–5252. [PubMed: 17404308]

31. Fujii E, Kato A, Chen YJ, Matsubara K, Ohnishi Y, Suzuki M: Characterization of EBV-related lymphoproliferative lesions arising in donor lymphocytes of transplanted human tumor tissues in the NOG mouse. Exp Anim2014:63(3):289–296. [PubMed: 25077758]
32. Gauvreau GM, Ellis AK, Denburg JA: Haemopoietic processes in allergic disease: eosinophil/basophil development. Clin Exp Allergy2009:39(9):1297–1306. [PubMed: 19622087]
33. Ghimire S, Weber D, Mavin E, Wang XN, Dickinson AM, Holler E: Pathophysiology of GvHD and Other HSCT-Related Major Complications. Front Immunol2017:8:79.
34. Gratton SM, Powell TR, Theeler BJ, Hawley JS, Amjad FS, Tornatore C: Neurological involvement and characterization in acquired hemophagocytic lymphohistiocytosis in adulthood. J Neurol Sci2015:357(1–2):136–142. [PubMed: 26198020]
35. Grom AA, Horne A, De Benedetti F: Macrophage Activation Syndrome in Rheumatic Diseases (MAS-HLH). In: Abla O, Janka G, eds. Histiocytic Disorders. Cham: Springer International Publishing; 2018: 233–246.
36. Gupta A, Weitzman S, Abdelhaleem M: The role of hemophagocytosis in bone marrow aspirates in the diagnosis of hemophagocytic lymphohistiocytosis. Pediatr Blood Cancer2008:50(2):192–194. [PubMed: 18061932]
37. Haddad E, Sulis ML, Jabado N, Blanche S, Fischer A, Tardieu M: Frequency and severity of central nervous system lesions in hemophagocytic lymphohistiocytosis. Blood1997:89(3):794–800. [PubMed: 9028310]
38. Hamilton JA: GM-CSF-Dependent Inflammatory Pathways. Frontiers in Immunology2019:10. [PubMed: 30723470]
39. Henter JI, Nennesmo I: Neuropathologic findings and neurologic symptoms in twenty-three children with hemophagocytic lymphohistiocytosis. J Pediatr1997:130(3):358–365. [PubMed: 9063409]
40. Henter JI, Samuelsson-Horne A, Arico M, Egeler RM, Elinder G, Filipovich AH, et al.: Treatment of hemophagocytic lymphohistiocytosis with HLH-94 immunochemotherapy and bone marrow transplantation. Blood2002:100(7):2367–2373. [PubMed: 12239144]
41. Horne A, Trottestam H, Arico M, Egeler RM, Filipovich AH, Gadner H, et al.: Frequency and spectrum of central nervous system involvement in 193 children with haemophagocytic lymphohistiocytosis. Br J Haematol2008:140(3):327–335. [PubMed: 18076710]
42. Huey DD, Bolon B, La Perle KMD, Kannian P, Jacobson S, Ratner L, et al.: Role of Wild-type and Recombinant Human T-cell Leukemia Viruses in Lymphoproliferative Disease in Humanized NSG Mice. Comp Med2018:68(1):4–14. [PubMed: 29460716]
43. Iacobucci I, Wen J, Meggendorfer M, Choi JK, Shi L, Pounds SB, et al.: Genomic subtyping and therapeutic targeting of acute erythroleukemia. Nat Genet2019:51(4):694–704. [PubMed: 30926971]
44. Ishikawa F, Yoshida S, Saito Y, Hijikata A, Kitamura H, Tanaka S, et al.: Chemotherapy-resistant human AML stem cells home to and engraft within the bone-marrow endosteal region. Nat Biotechnol2007:25(11):1315–1321. [PubMed: 17952057]
45. Janka GE, Lehmberg K: Hemophagocytic syndromes--an update. Blood Rev2014:28(4):135–142. [PubMed: 24792320]
46. Jessen B, Kogl T, Sepulveda FE, de Saint Basile G, Aichele P, Ehl S: Graded defects in cytotoxicity determine severity of hemophagocytic lymphohistiocytosis in humans and mice. Front Immunol2013:4:448. [PubMed: 24379813]
47. Johanna I, Straetemans T, Heijhuurs S, Aarts-Riemens T, Norell H, Bongiovanni L, et al.: Evaluating in vivo efficacy – toxicity profile of TEG001 in humanized mice xenografts against primary human AML disease and healthy hematopoietic cells. Journal for ImmunoTherapy of Cancer2019:7(1):69. [PubMed: 30871629]
48. Jordan MB, Allen CE, Greenberg J, Henry M, Hermiston ML, Kumar A, et al.: Challenges in the diagnosis of hemophagocytic lymphohistiocytosis: Recommendations from the North American Consortium for Histiocytosis (NACHO). Pediatr Blood Cancer2019:e27929. [PubMed: 31339233]

49. Ju HY, Hong CR, Kim SJ, Lee JW, Kim H, Kang HJ, et al.: Hemophagocytic lymphohistiocytosis diagnosed by brain biopsy. Korean J Pediatr2015:58(9):358–361. [PubMed: 26512263]
50. Kim HJ, Ko YH, Kim JE, Lee SS, Lee H, Park G, et al.: Epstein-Barr Virus-Associated Lymphoproliferative Disorders: Review and Update on 2016 WHO Classification. J Pathol Transl Med2017:51(4):352–358. [PubMed: 28592786]
51. Kirshenbaum AS, Goff JP, Dreskin SC, Irani AM, Schwartz LB, Metcalfe DD: IL-3-dependent growth of basophil-like cells and mastlike cells from human bone marrow. J Immunol1989:142(7):2424–2429. [PubMed: 2647850]
52. Kirshenbaum AS, Goff JP, Kessler SW, Mican JM, Zsebo KM, Metcalfe DD: Effect of IL-3 and stem cell factor on the appearance of human basophils and mast cells from CD34+ pluripotent progenitor cells. J Immunol1992:148(3):772–777. [PubMed: 1370517]
53. Klein C, Kleinschmidt-DeMasters BK, Liang X, Stence N, Tuder RM, Moore BE: A Review of Neuropathological Features of Familial and Adult Hemophagocytic Lymphohistiocytosis. J Neuropathol Exp Neurol2019:78(3):197–208. [PubMed: 30726926]
54. Kogl T, Muller J, Jessen B, Schmitt-Graeff A, Janka G, Ehl S, et al.: Hemophagocytic lymphohistiocytosis in syntaxin-11-deficient mice: T-cell exhaustion limits fatal disease. Blood2013:121(4):604–613. [PubMed: 23190531]
55. Lang RA, Metcalf D, Cuthbertson RA, Lyons I, Stanley E, Kelso A, et al.: Transgenic mice expressing a hemopoietic growth factor gene (GM-CSF) develop accumulations of macrophages, blindness, and a fatal syndrome of tissue damage. Cell1987:51(4):675–686. [PubMed: 3499986]
56. Lee WY, Weinberg OK, Pinkus GS: GATA1 Is a Sensitive and Specific Nuclear Marker for Erythroid and Megakaryocytic Lineages. Am J Clin Pathol2017:147(4):420–426. [PubMed: 28340113]
57. Lin S, Luo RT, Shrestha M, Thirman MJ, Mulloy JC: The full transforming capacity of MLL-Af4 is interlinked with lymphoid lineage commitment. Blood2017:130(7):903–907. [PubMed: 28637661]
58. Lockridge JL, Zhou Y, Becker YA, Ma S, Kenney SC, Hematti P, et al.: Mice engrafted with human fetal thymic tissue and hematopoietic stem cells develop pathology resembling chronic graft-versus-host disease. Biol Blood Marrow Transplant2013:19(9):1310–1322. [PubMed: 23806772]
59. Lopez AF, Begley CG, Williamson DJ, Warren DJ, Vadas MA, Sanderson CJ: Murine eosinophil differentiation factor. An eosinophil-specific colony-stimulating factor with activity for human cells. J Exp Med1986:163(5):1085–1099. [PubMed: 3486243]
60. Malaise M, Neumeier M, Botteron C, Dohner K, Reinhardt D, Schlegelberger B, et al.: Stable and reproducible engraftment of primary adult and pediatric acute myeloid leukemia in NSG mice. Leukemia2011:25(10):1635–1639. [PubMed: 21647161]
61. Martinez-Moczygemba M, Huston DP: Biology of common beta receptor-signaling cytokines: IL-3, IL-5, and GM-CSF. J Allergy Clin Immunol2003:112(4):653–665; quiz 666. [PubMed: 14564341]
62. McDermott SP, Eppert K, Lechman ER, Doedens M, Dick JE: Comparison of human cord blood engraftment between immunocompromised mouse strains. Blood2010:116(2):193–200. [PubMed: 20404133]
63. Metcalf D, Begley CG, Johnson GR, Nicola NA, Lopez AF, Williamson DJ: Effects of purified bacterially synthesized murine multi-CSF (IL-3) on hematopoiesis in normal adult mice. Blood1986:68(1):46–57. [PubMed: 3087441]
64. Morscio J, Tousseyn T: Recent insights in the pathogenesis of post-transplantation lymphoproliferative disorders. World J Transplant2016:6(3):505–516. [PubMed: 27683629]
65. Murray PJ, Allen JE, Biswas SK, Fisher EA, Gilroy DW, Goerdt S, et al.: Macrophage activation and polarization: nomenclature and experimental guidelines. Immunity2014:41(1):14–20. [PubMed: 25035950]
66. Na YR, Jung D, Gu GJ, Seok SH: GM-CSF Grown Bone Marrow Derived Cells Are Composed of Phenotypically Different Dendritic Cells and Macrophages. Mol Cells2016:39(10):734–741. [PubMed: 27788572]

67. Nicolini FE, Cashman JD, Hogge DE, Humphries RK, Eaves CJ: NOD/SCID mice engineered to express human IL-3, GM-CSF and Steel factor constitutively mobilize engrafted human progenitors and compromise human stem cell regeneration. Leukemia2004:18(2):341–347. [PubMed: 14628073]
68. Pham NL, Badovinac VP, Harty JT: Epitope specificity of memory CD8+ T cells dictates vaccination-induced mortality in LCMV-infected perforin-deficient mice. Eur J Immunol2012:42(6):1488–1499. [PubMed: 22678903]
69. Radaelli E, Hermans E, Omodho L, Francis A, Vander Borght S, Marine JC, et al.: Spontaneous Post-Transplant Disorders in NOD.Cg- Prkdcscid Il2rgtm1Sug/JicTac (NOG) Mice Engrafted with Patient-Derived Metastatic Melanomas. PLoS One2015:10(5):e0124974. [PubMed: 25996609]
70. Ramos-Casals M, Brito-Zeron P, Lopez-Guillermo A, Khamashta MA, Bosch X: Adult haemophagocytic syndrome. Lancet2014:383(9927):1503–1516. [PubMed: 24290661]
71. Ravelli A, Grom AA, Behrens EM, Cron RQ: Macrophage activation syndrome as part of systemic juvenile idiopathic arthritis: diagnosis, genetics, pathophysiology and treatment. Genes Immun2012:13(4):289–298. [PubMed: 22418018]
72. Rezk SA UN, Woda BA: Non-neoplastic Histiocytic Proliferations of Lymph Nodes and Bone Marrow. In: Jaffe ESAD, Campo E, Harris NL, Quintanilla-Fend L, ed. Hematopathology. Philadelphia, PA: Elsevier; 2017: 957–968.
73. Risti B, Flury RF, Schaffner A: Fatal hematophagic histiocytosis after granulocyte-macrophage colony-stimulating factor and chemotherapy for high-grade malignant lymphoma. Clin Investig1994:72(6):457–461.
74. Rosato RR, Davila-Gonzalez D, Choi DS, Qian W, Chen W, Kozielski AJ, et al.: Evaluation of anti-PD-1-based therapy against triple-negative breast cancer patient-derived xenograft tumors engrafted in humanized mouse models. Breast Cancer Res2018:20(1):108. [PubMed: 30185216]
75. Rouphael NG, Talati NJ, Vaughan C, Cunningham K, Moreira R, Gould C: Infections associated with haemophagocytic syndrome. Lancet Infect Dis2007:7(12):814–822. [PubMed: 18045564]
76. Saito H, Ebisawa M, Tachimoto H, Shichijo M, Fukagawa K, Matsumoto K, et al.: Selective growth of human mast cells induced by Steel factor, IL-6, and prostaglandin E2 from cord blood mononuclear cells. J Immunol1996:157(1):343–350. [PubMed: 8683136]
77. Schroeder MA, DiPersio JF: Mouse models of graft-versus-host disease: advances and limitations. Dis Model Mech2011:4(3):318–333. [PubMed: 21558065]
78. Schulert GS, Minoia F, Bohnsack J, Cron RQ, Hashad S, KonÉ-Paut I, et al.: Effect of Biologic Therapy on Clinical and Laboratory Features of Macrophage Activation Syndrome Associated With Systemic Juvenile Idiopathic Arthritis. Arthritis Care & Research2018:70(3):409–419. [PubMed: 28499329]
79. Shimoda K, Okamura S, Harada N, Niho Y: Detection of the granulocyte colony-stimulating factor receptor using biotinylated granulocyte colony-stimulating factor: presence of granulocyte colony-stimulating factor receptor on CD34-positive hematopoietic progenitor cells. Res Exp Med (Berl)1992:192(4):245–255. [PubMed: 1384092]
80. Shultz LD, Keck J, Burzenski L, Jangalwe S, Vaidya S, Greiner DL, et al.: Humanized mouse models of immunological diseases and precision medicine. Mamm Genome2019:30(5–6):123–142. [PubMed: 30847553]
81. Shultz LD, Lyons BL, Burzenski LM, Gott B, Chen X, Chaleff S, et al.: Human lymphoid and myeloid cell development in NOD/LtSz-scid IL2R gamma null mice engrafted with mobilized human hemopoietic stem cells. J Immunol2005:174(10):6477–6489. [PubMed: 15879151]
82. Siolas D, Hannon GJ: Patient-derived tumor xenografts: transforming clinical samples into mouse models. Cancer Res2013:73(17):5315–5319. [PubMed: 23733750]
83. Sonntag K, Eckert F, Welker C, Muller H, Muller F, Zips D, et al.: Chronic graft-versus-host-disease in CD34(+)-humanized NSG mice is associated with human susceptibility HLA haplotypes for autoimmune disease. J Autoimmun2015:62:55–66. [PubMed: 26143958]
84. Spath S, Komuczki J, Hermann M, Pelczar P, Mair F, Schreiner B, et al.: Dysregulation of the Cytokine GM-CSF Induces Spontaneous Phagocyte Invasion and Immunopathology in the Central Nervous System. Immunity2017:46(2):245–260. [PubMed: 28228281]

85. Stepp SE, Dufourcq-Lagelouse R, Le Deist F, Bhawan S, Certain S, Mathew PA, et al.: Perforin gene defects in familial hemophagocytic lymphohistiocytosis. Science1999:286(5446):1957–1959. [PubMed: 10583959]

86. Stripecke R, Munz C, Schuringa JJ, Bissig KD, Soper B, Meeham T, et al.: Innovations, challenges, and minimal information for standardization of humanized mice. EMBO Mol Med2020:12(7):e8662. [PubMed: 32578942]

87. Takagi S, Saito Y, Hijikata A, Tanaka S, Watanabe T, Hasegawa T, et al.: Membrane-bound human SCF/KL promotes in vivo human hematopoietic engraftment and myeloid differentiation. Blood2012:119(12):2768–2777. [PubMed: 22279057]

88. Tillman H, Vogel P, Rogers T, Akers W, Rehg JE: Spectrum of Posttransplant Lymphoproliferations in NSG Mice and Their Association With EBV Infection After Engraftment of Pediatric Solid Tumors. Vet Pathol2020:57(3):445–456. [PubMed: 32202225]

89. Tran HT, Metcalf D, Cheers C: Anti-bacterial activity of peritoneal cells from transgenic mice producing high levels of GM-CSF. Immunology1990:71(3):377–382. [PubMed: 2269477]

90. Ushach I, Zlotnik A: Biological role of granulocyte macrophage colony-stimulating factor (GM-CSF) and macrophage colony-stimulating factor (M-CSF) on cells of the myeloid lineage. J Leukoc Biol2016:100(3):481–489. [PubMed: 27354413]

91. van Diggelen OP, Shin SI, Phillips DM: Reduction in cellular tumorigenicity after mycoplasma infection and elimination of mycoplasma from infected cultures by passage in nude mice. Cancer Res1977:37(8 Pt 1):2680–2687. [PubMed: 872095]

92. van Nieuwenhuijze AE, Coghill E, Gray D, Prato S, Metcalf D, Alexander WS, et al.: Transgenic expression of GM-CSF in T cells causes disseminated histiocytosis. Am J Pathol2014:184(1):184–199. [PubMed: 24183847]

93. Wang M, Yao LC, Cheng M, Cai D, Martinek J, Pan CX, et al.: Humanized mice in studying efficacy and mechanisms of PD-1-targeted cancer immunotherapy. FASEB J2018:32(3):1537–1549. [PubMed: 29146734]

94. Wang S, Degar BA, Zieske A, Shafi NQ, Rose MG: Hemophagocytosis exacerbated by G-CSF/GM-CSF treatment in a patient with myelodysplasia. Am J Hematol2004:77(4):391–396. [PubMed: 15551287]

95. Wei J, Wunderlich M, Fox C, Alvarez S, Cigudosa JC, Wilhelm JS, et al.: Microenvironment determines lineage fate in a human model of MLL-AF9 leukemia. Cancer Cell2008:13(6):483–495. [PubMed: 18538732]

96. Williams SA, Anderson WC, Santaguida MT, Dylla SJ: Patient-derived xenografts, the cancer stem cell paradigm, and cancer pathobiology in the 21st century. Lab Invest2013:93(9):970–982. [PubMed: 23917877]

97. Wunderlich M, Chou FS, Link KA, Mizukawa B, Perry RL, Carroll M, et al.: AML xenograft efficiency is significantly improved in NOD/SCID-IL2RG mice constitutively expressing human SCF, GM-CSF and IL-3. Leukemia2010:24(10):1785–1788. [PubMed: 20686503]

98. Wunderlich M, Chou FS, Sexton C, Presicce P, Chougnet CA, Aliberti J, et al.: Improved multilineage human hematopoietic reconstitution and function in NSGS mice. PLoS One2018:13(12):e0209034. [PubMed: 30540841]

99. Wunderlich M, Stockman C, Devarajan M, Ravishankar N, Sexton C, Kumar AR, et al.: A xenograft model of macrophage activation syndrome amenable to anti-CD33 and anti-IL-6R treatment. JCI Insight2016:1(15):e88181. [PubMed: 27699249]

100. Yoshihara S, Li Y, Xia J, Danzl N, Sykes M, Yang YG: Posttransplant Hemophagocytic Lymphohistiocytosis Driven by Myeloid Cytokines and Vicious Cycles of T-Cell and Macrophage Activation in Humanized Mice. Front Immunol2019:10:186. [PubMed: 30814997]

101. Zella D, Curreli S, Benedetti F, Krishnan S, Cocchi F, Latinovic OS, et al.: Mycoplasma promotes malignant transformation in vivo, and its DnaK, a bacterial chaperone protein, has broad oncogenic properties. Proc Natl Acad Sci U S A2018:115(51):E12005–E12014. [PubMed: 30509983]

102. Zhan Y, Lew AM, Chopin M: The Pleiotropic Effects of the GM-CSF Rheostat on Myeloid Cell Differentiation and Function: More Than a Numbers Game. Front Immunol2019:10:2679. [PubMed: 31803190]

103. Zhang L, Liu Y, Wang X, Tang Z, Li S, Hu Y, et al.: The extent of inflammatory infiltration in primary cancer tissues is associated with lymphomagenesis in immunodeficient mice. Sci Rep2015:5:9447. [PubMed: 25819560]

104. Zhang Y, He L, Selimoglu-Buet D, Jego C, Morabito M, Willekens C, et al.: Engraftment of chronic myelomonocytic leukemia cells in immunocompromised mice supports disease dependency on cytokines. Blood Adv2017:1(14):972–979. [PubMed: 29296739]

105. Zoller EE, Lykens JE, Terrell CE, Aliberti J, Filipovich AH, Henson PM, et al.: Hemophagocytosis causes a consumptive anemia of inflammation. J Exp Med2011:208(6):1203–1214. [PubMed: 21624938]

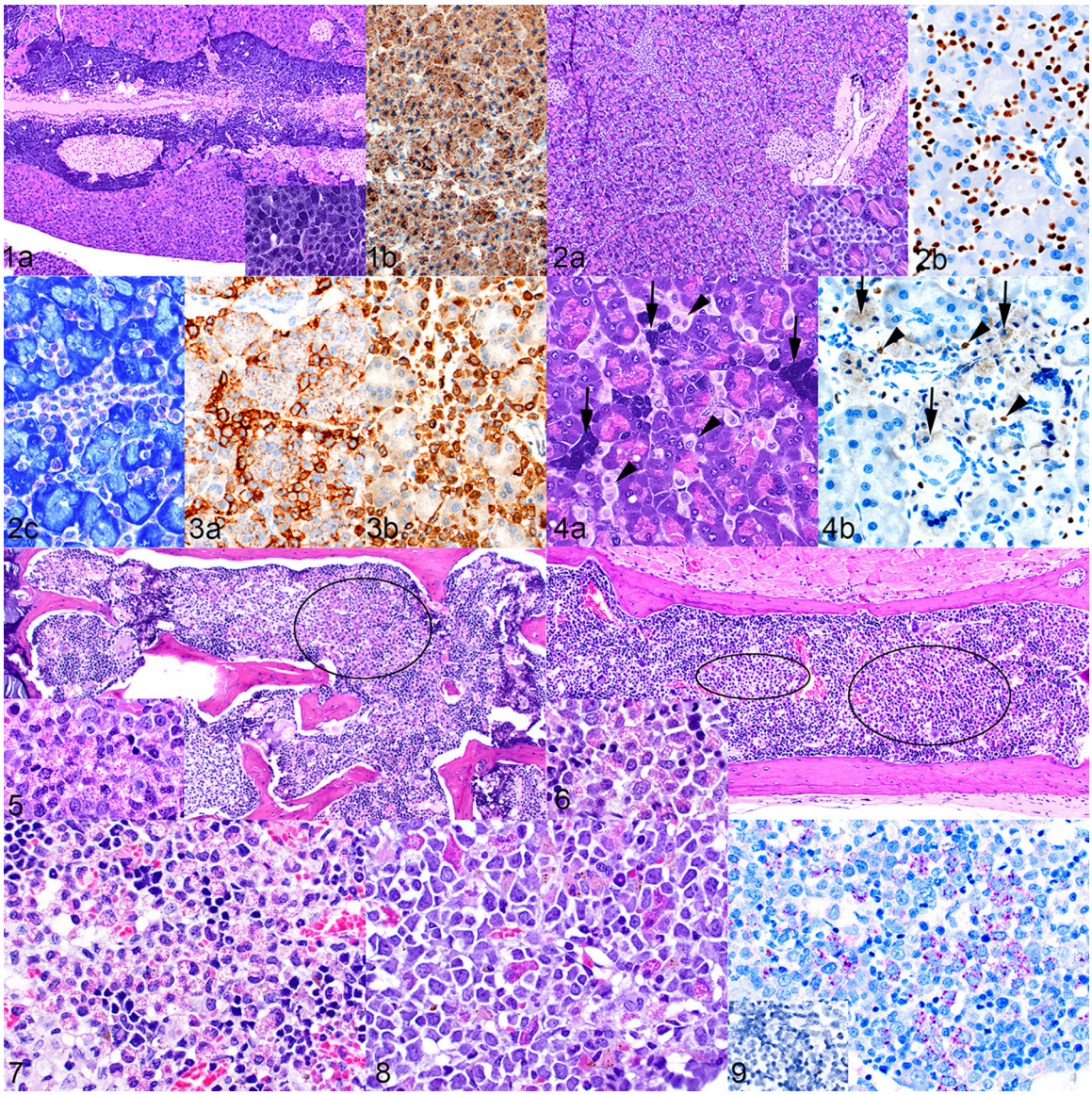

Figures 1–9.

Figure 1. Mast cell hyperplasia, pancreas, naïve mouse. (a) Large aggregates of mast cells surround the pancreatic ducts and adjacent islets. Inset: there is a high level of granulation in these cells. Hematoxylin and eosin (HE). (b) The absence of nuclear labeling with antibody to hNuMA1 indicates that the cells are of mouse origin. The cytoplasmic color is non-specific staining due to mast cell granules. **Figure 2.** Mast cell hyperplasia, pancreas, mouse implanted with transduced hCD34+ cells (mouse no. 15). (a) Interstitial infiltrates of mast cells are present throughout the pancreas. Inset: the mast cells are smaller, have fewer granules and are paler when compared to the mouse mast cells in Figure 1. (b) Positive nuclear labeling with antibody to hNuMA1 indicates that these cells are of human origin. (c) Metachromatic staining of granules with toluidine blue supports the identification of the cells as mast cells. **Figure 3.** Mast cell hyperplasia, pancreas, humanized mouse (mouse no. 10). The identity of the mast cells is confirmed by positive labeling for c-Kit/CD117

(a) and mast cell tryptase (b). **Figure 4.** Mast cell hyperplasia, pancreas, mouse implanted with an acute erythroid leukemia (AEL) xenograft (mouse no. 20). (a) The pancreas contains both foci of large highly granulated mouse mast cells (arrows) and interstitial infiltrates of smaller, more lightly granulated human mast cells (arrowheads). HE. (b) The human cells show positive nuclear labeling for hNuMA1 (arrowheads), and the mouse cells are negative for nuclear hNuMA1 (arrows). **Figure 5.** Eosinophil hyperplasia, bone marrow of vertebra, humanized mouse (mouse no. 1). The bone marrow contains patchy areas with markedly increased numbers of eosinophil precursors (example area circled). Inset: cellular detail of eosinophil granules. HE. **Figure 6.** Eosinophil hyperplasia, bone marrow of sternum, mouse implanted with transduced hCD34+ cells (mouse no. 15). The circled areas indicate patches of eosinophil precursors and the inset shows cellular detail. HE. **Figure 7.** Eosinophil hyperplasia, bone marrow of sternum, mouse implanted with an AEL patient-derived xenograft (PDX). HE. **Figure 8.** Eosinophil hyperplasia, bone marrow of sternum, mouse implanted with an AML PDX. HE. **Figure 9.** Immunohistochemical labeling of a section from the mouse in Figure 6. The cells are confirmed to be of human eosinophilic lineage by positive labeling for the human-specific major basic protein (MBP). Inset: no labeling for mouse-specific MBP.

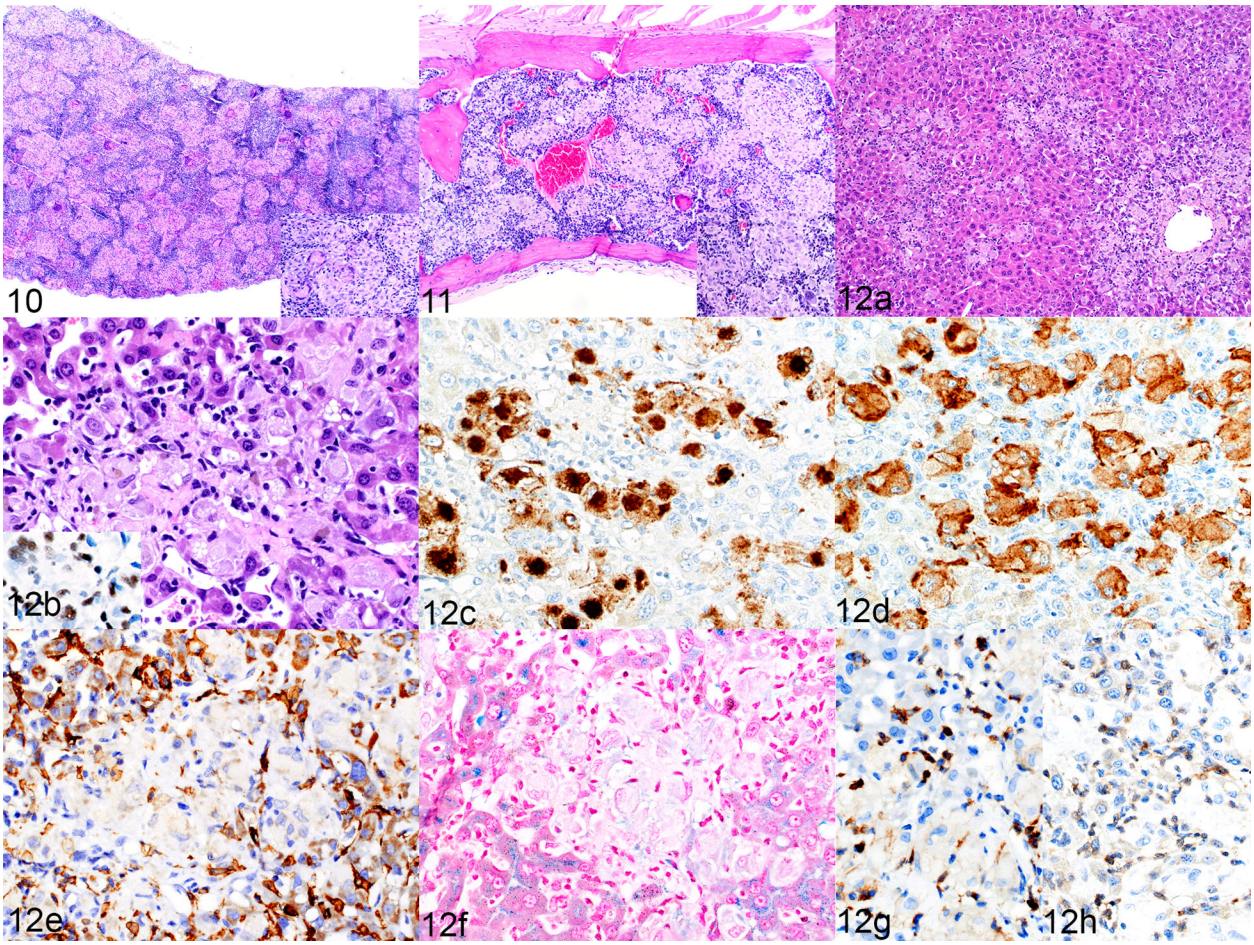

Figures 10–12.

Figures 10 and 11. Histiocytosis, spleen (Figure 10) and bone marrow (Figure 11), NSG mouse implanted with transduced hCD34+ cells (mouse no. 25). HE. **Figure 12.** Histiocytosis, liver, NSG mouse implanted with a B-ALL patient-derived xenograft (mouse no 27). (a) Multifocal aggregates of macrophages are randomly scattered throughout the liver. HE. (b) The large cells have abundant cytoplasm. HE. Inset: positive immunolabeling for hNuMA1, confirming the human origin of the cells. (c–e) Macrophages are positive for hCD68 (c) and hCD163 (d), and the aggregates are surrounded by hyperplastic F4/80-positive mouse cells (e). (f) Iron is not detected in the macrophage cytoplasm. Prussian blue. (g, h) Scattered among the macrophages are small numbers of small cells immunolabeled for hCD45 (g) and CD3 (h).

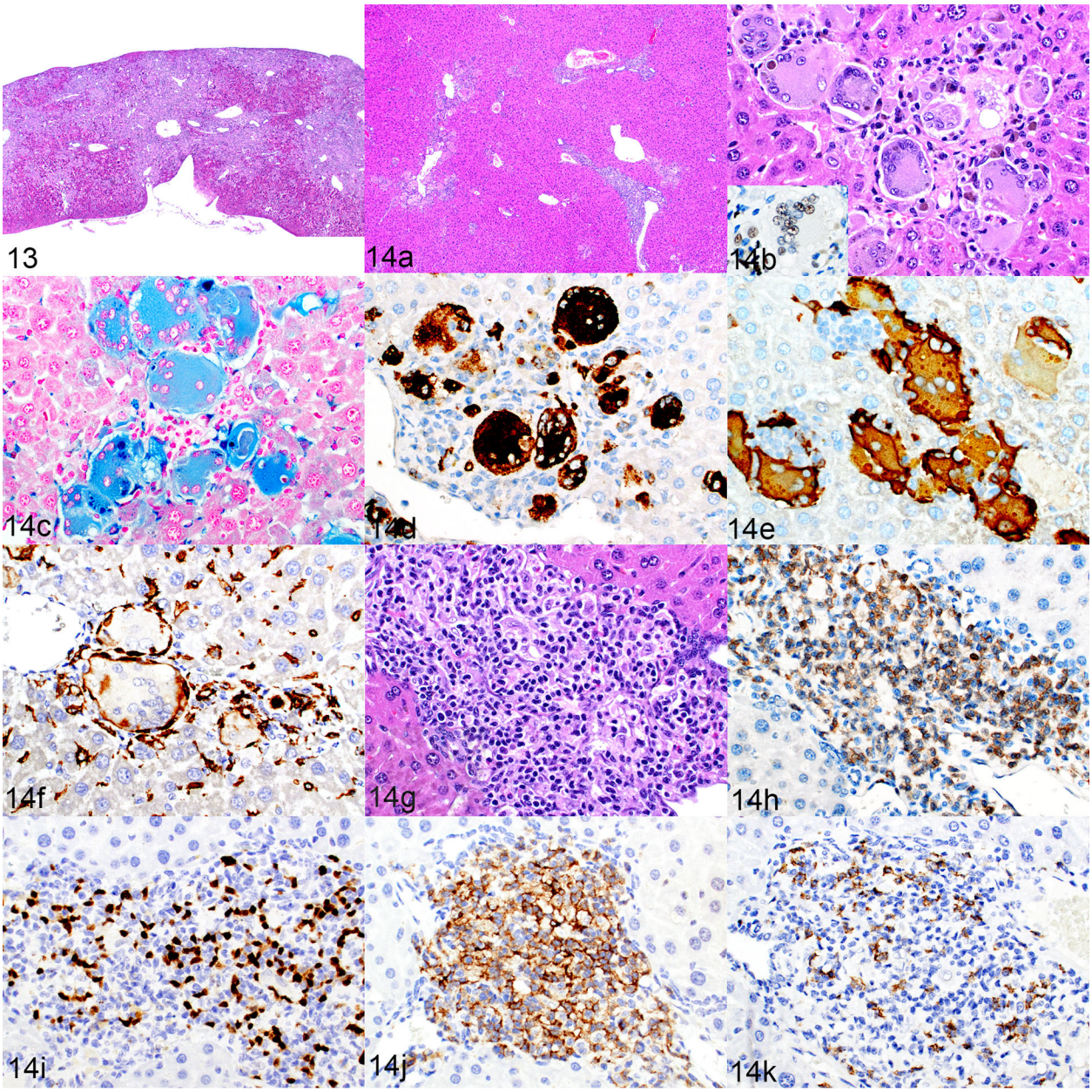

Figures 13 and 14.

Macrophage and lymphocyte infiltrates, liver, humanized NSG-SGM3 mice. **Figure 13.** Mouse no. 13. Severe macrophage and lymphocyte infiltration with replacement of the liver parenchyma and grossly visible compaction. HE. **Figure 14.** Mouse no. 2. Morphologic and immunophenotypic characterization of liver infiltrates representative of typical moderate severity. (a) Mild to moderate portal, perivascular and sinusoidal infiltrates. Same magnification as Fig. 13. HE. Figures 14 b–f show higher magnification of the macrophage area in Fig 14a, and Figs 14 g–k show the lymphoid area. (b) The cells are predominantly large multinucleated giant cells with intracytoplasmic pigment. HE. Inset: the cells are hNuMA1-positive. (c–e) The cytoplasm of these macrophages stains positively for iron with Prussian Blue (c) and is immunolabeled for hCD68 (d) and hCD163 (e). (f)

Individual large multinucleated giant cells are surrounded by cells that are immunolabeled for mouse F4/80. (g) A portal area of liver infiltrated by lymphocytes. HE. (h–k) The lymphoid population contains slightly more CD3-positive T cells (h) than PAX5-positive B cells (i). The T-cell population is predominately CD4-positive (j) but includes low numbers of CD8-positive cells (k).

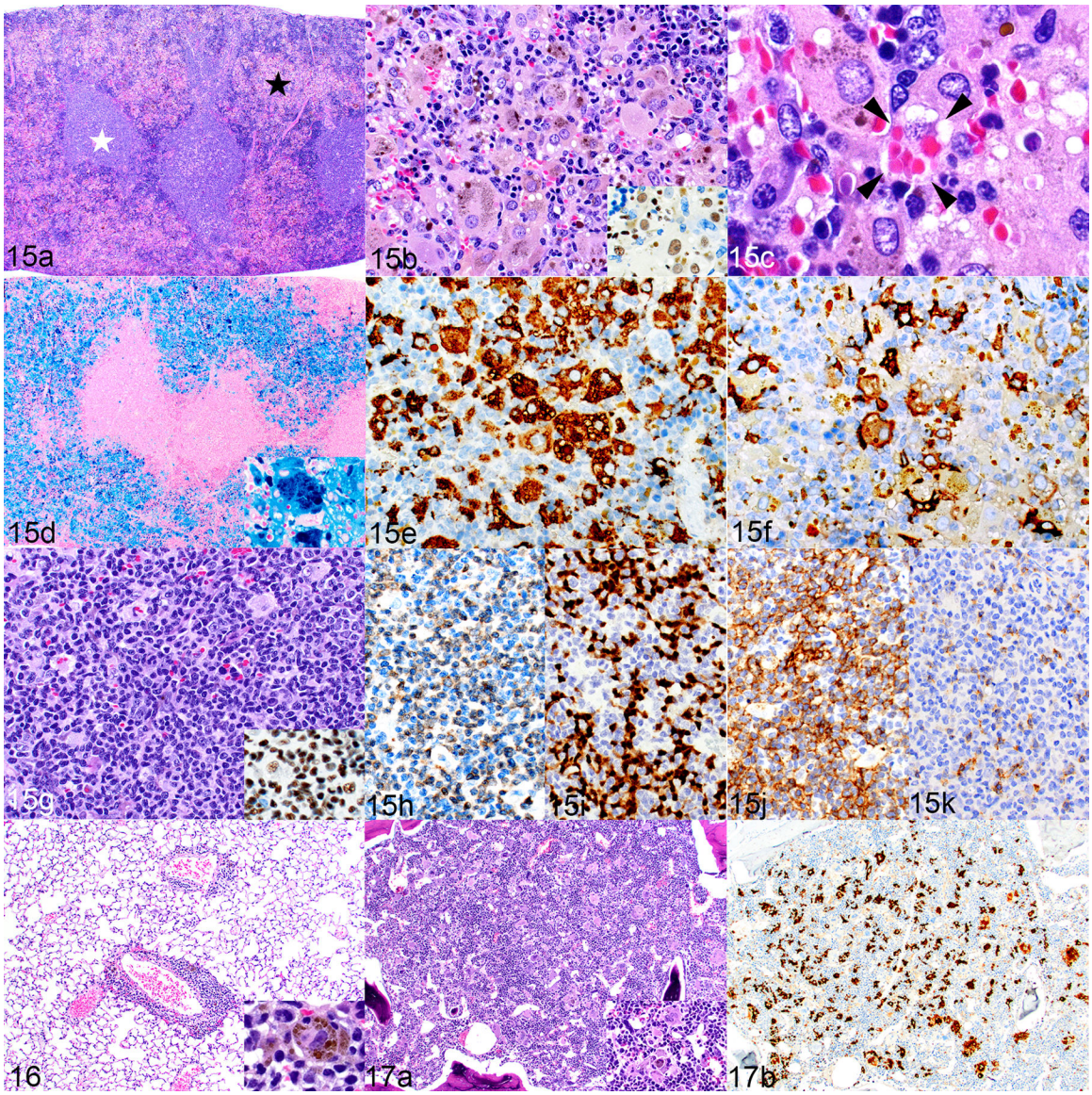

Figures 15–17.

Histiocytosis, hemophagocytosis, and human lymphocyte engraftment; humanized NSG-SGM3 mouse (mouse no. 2). **Figure 15.** Spleen. (a) There is a visible distinction between the white pulp (white star) and red pulp (black star). HE. (b) The red pulp area contains numerous large macrophages with abundant cytoplasm and frequent cytoplasmic pigment. HE. Inset: the cells are immunolabeled for hNuMA1. (c) Hemophagocytosis is occasionally indicated by engulfed erythrocytes in the macrophage cytoplasm (bounded by arrowheads). HE. (d) Marked hemophagocytosis and iron accumulation (inset). Prussian blue. (e-k). Most of the macrophages are immunolabeled for hCD68 (e), with fewer being positive for hCD163 (f). The white pulp is populated by human lymphocytes, based on morphology with HE stain (g) and positive labeling for hNuMA1 (inset). The white pulp contains similar numbers of CD3-positive T cells (h) and PAX5-positive B cells (i). Most of the T cells are CD4 positive (j) with fewer CD8-positive cells (k). **Figure 16**. Lung. There is minimal to

mild perivascular infiltration of lymphocytes and histiocytes. The histiocytes occasionally contain intracytoplasmic pigment (inset). **Figure 17**. Bone marrow. (a) Large histiocytes and multinucleated giant cells are scattered throughout the bone marrow, occasionally containing intracytoplasmic pigment (inset). HE. (b) The histiocytes are immunolabeled for hCD68.

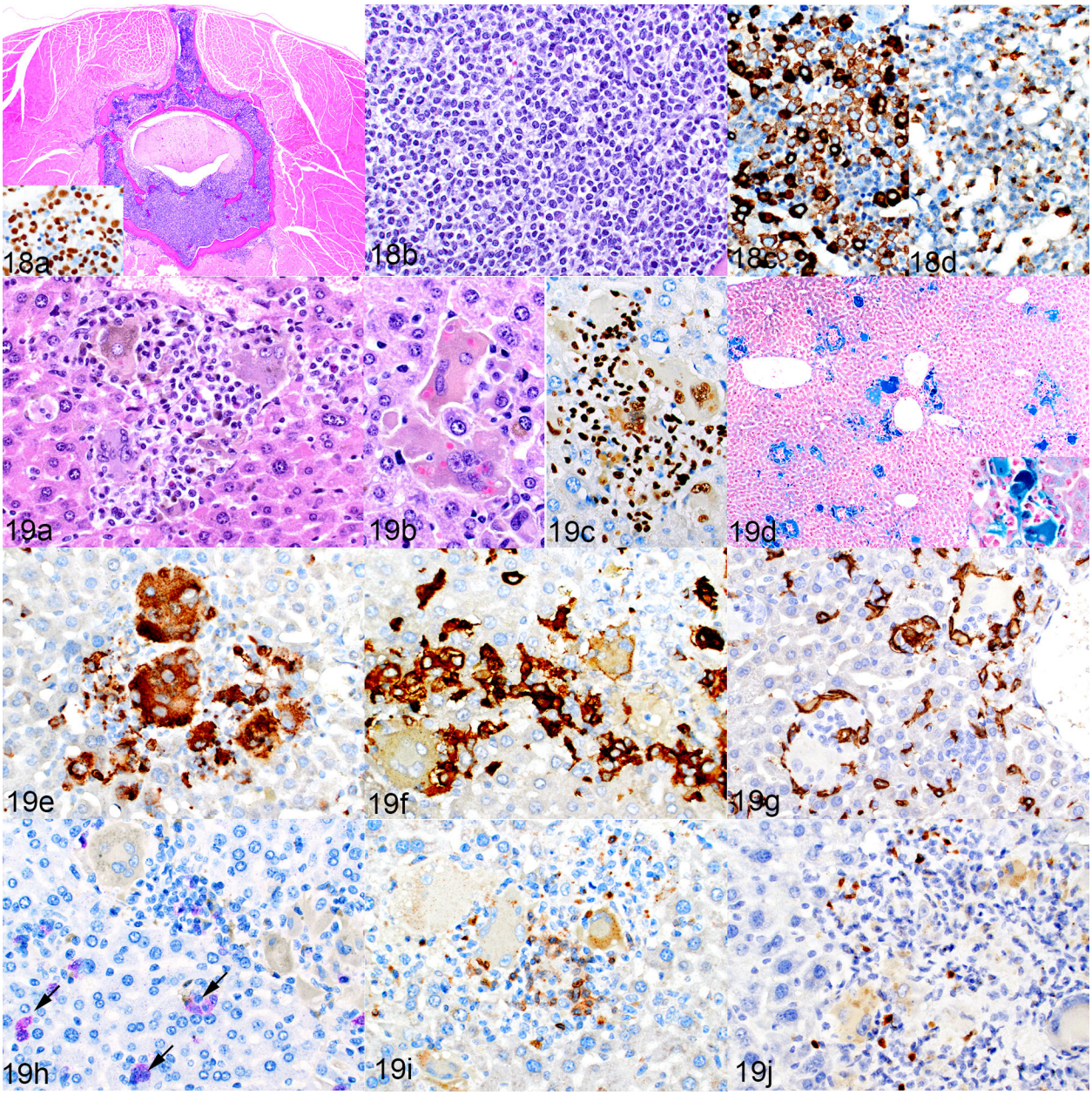

Figures 18 and 19.

NSG-SGM3 mice implanted with transduced hCD34-positive cells. **Figure 18.** Leukemia, bone marrow, mouse no. 15. (a,b) A cross-section of a vertebra, with replacement of the marrow by leukemic cells, which infiltrate into the epidural space and surrounding muscle. HE. Inset: the leukemic cells are hNuMA-positive. The leukemia is myelomonocytic, as indicated by positivity for MPO (c) and hCD68 (d). **Figure 19.** Leukemia as well as macrophage and lymphocyte infiltrates, liver, . (a) There are aggregates of large macrophages with cytoplasmic pigment, and admixed small lymphocytic cells. HE. (b) Intracytoplasmic erythrocytes indicative of erythrophagocytosis. (c) The lymphocytes and macrophages are immunolabeled for hNuMA1. (d) Multiple aggregates of macrophages containing blue-staining iron. Inset: higher magnification. Prussian blue. (e–h) These cells

are positive for hCD68 (e) and hCD163 (f) and are rimmed by mouse F4/80-positive cells (g), similar to the cells of the humanized mice in Figure 14. Occasional GFP-positive leukemia cells are present in the liver sinusoids (h, purple chromogen, arrows). (i, j) Admixed with the macrophages are low numbers of CD3-positive T cells (i) and PAX5-positive B cells (j).

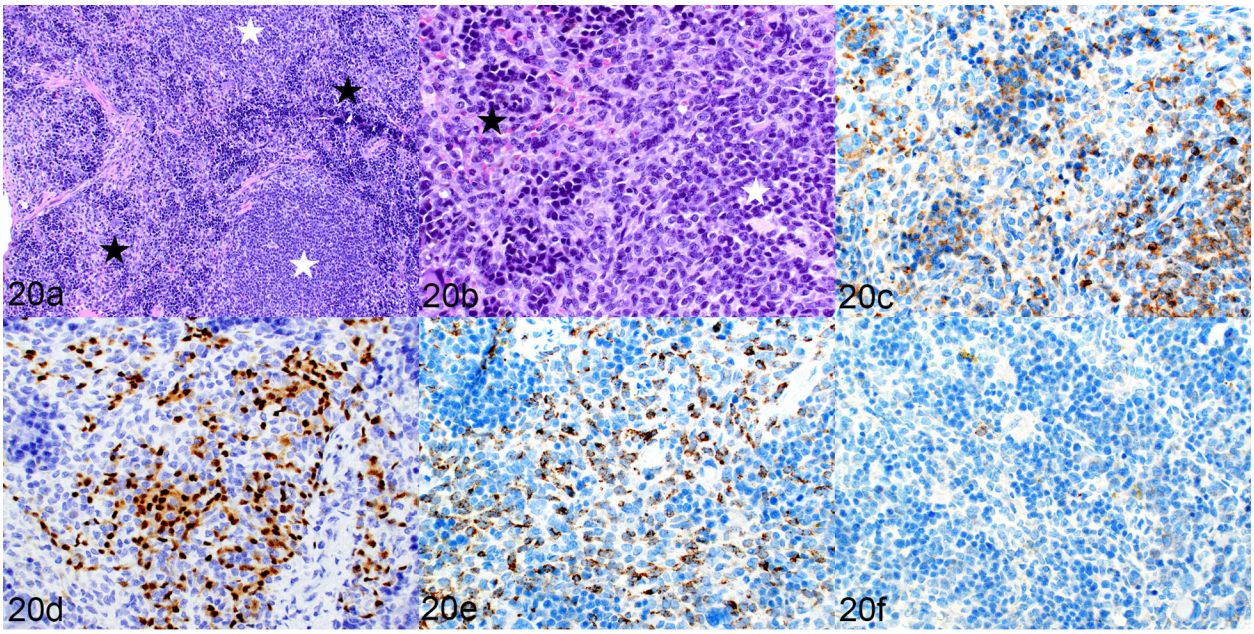

Figure 20.

Engraftment of human leukemic cells and human lymphocytes, spleen, mouse implanted with transduced hCD34+ cells (mouse no. 17). (a) White starred areas indicate white pulp areas, black stars indicate red pulp. (b) The white pulp is populated by small lymphoid cells and the red pulp contains myeloid cells and extramedullary hematopoiesis. HE. (c–f) The white pulp contains a mixture of CD3-positive T cells (c) and PAX5-positive B cells (d). The myeloid cells in the red pulp are positive for hCD68 (e) and negative for hCD163 (f).

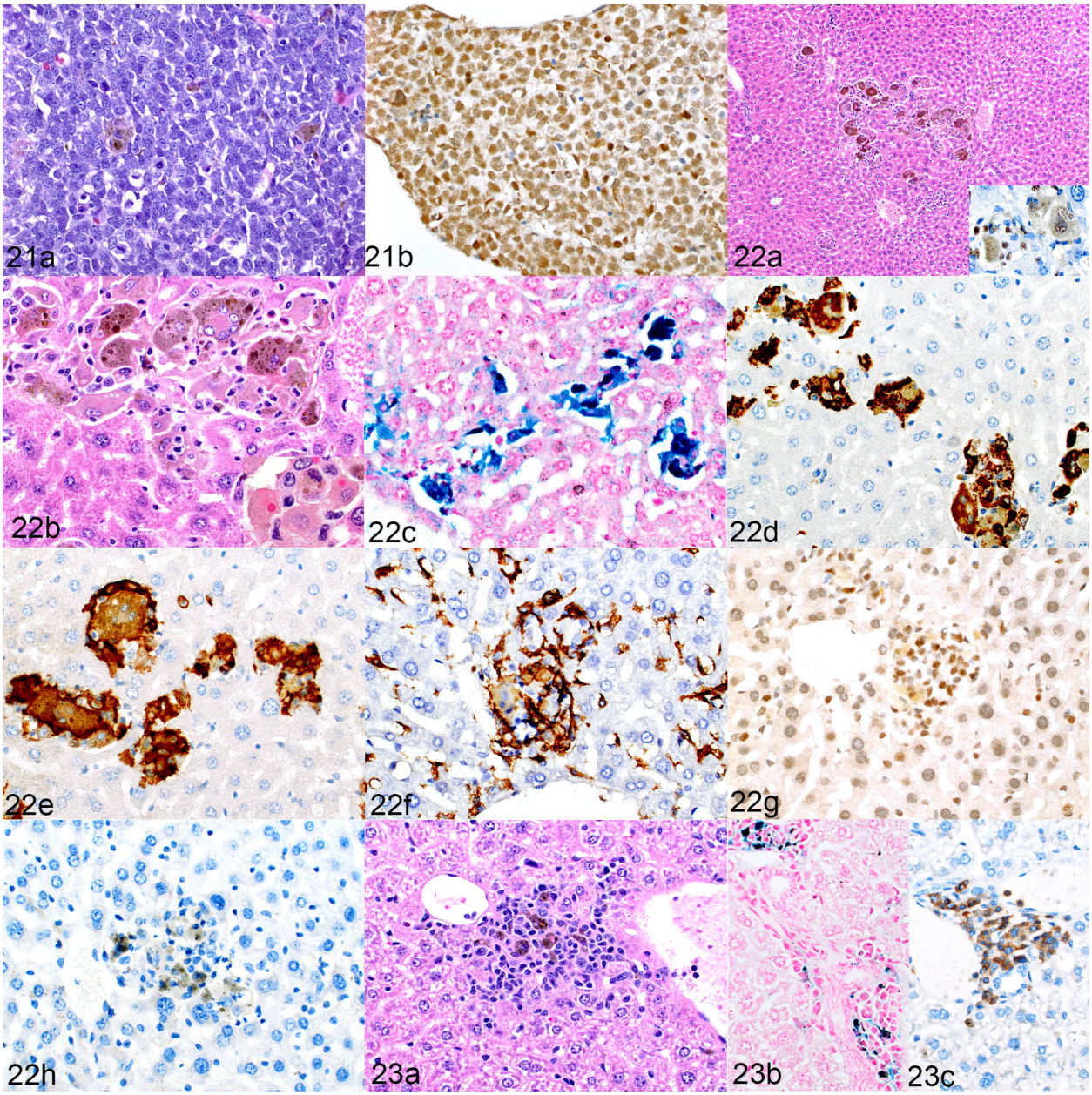

Figures 21–23.

NSG-SGM3 mice implanted with acute erythroid leukemia (AEL) patient-derived xenografts (PDX). **Figures 21 and 22.** Engraftment of human leukemia cells, mouse no. 20. **Figure 21.** Bone marrow. (a) The marrow is filled with a homogeneous population of leukemic cells and occasional, scattered pigment-containing macrophages. HE. (b) The erythroid leukemic cells are positive for GATA1. **Figure 22.** Macrophage proliferation, liver. (a) There are aggregates of large macrophages with prominent cytoplasmic pigment. HE. Inset: cells are positive for hNuMA1. (b) The cells include multinucleated giant cells. Inset: intracytoplasmic erythocytes indicating erythrophagocytosis. HE. (c) The cytoplasmic pigment stains positively for iron. Prussian blue. (d–h) The cells are immunolabeled for hCD68 (d) and hCD163 (e) and are surrounded by mouse F4/80-positive cells (f). Admixed

within these aggregates are low numbers of leukemic cells, identified by positive GATA1 labeling (g). Surprisingly, this mouse showed no CD3-positive T cells (h); the brown pigment in the image is iron, not immunolabeling. **Figure 23.**Macrophage proliferation, hemophagocytosis, and lymphocytic proliferation; liver, mouse implanted with an AEL PDX in which the leukemia did not engraft (mouse no. 19). (a) The liver contains mixed aggregates of macrophages (with cytoplasmic pigment) and small lymphocytes. HE. (b) The cytoplasmic pigment stains positively for iron. Prussian blue. (c) Low to moderate numbers of CD3-positive T cells are present.

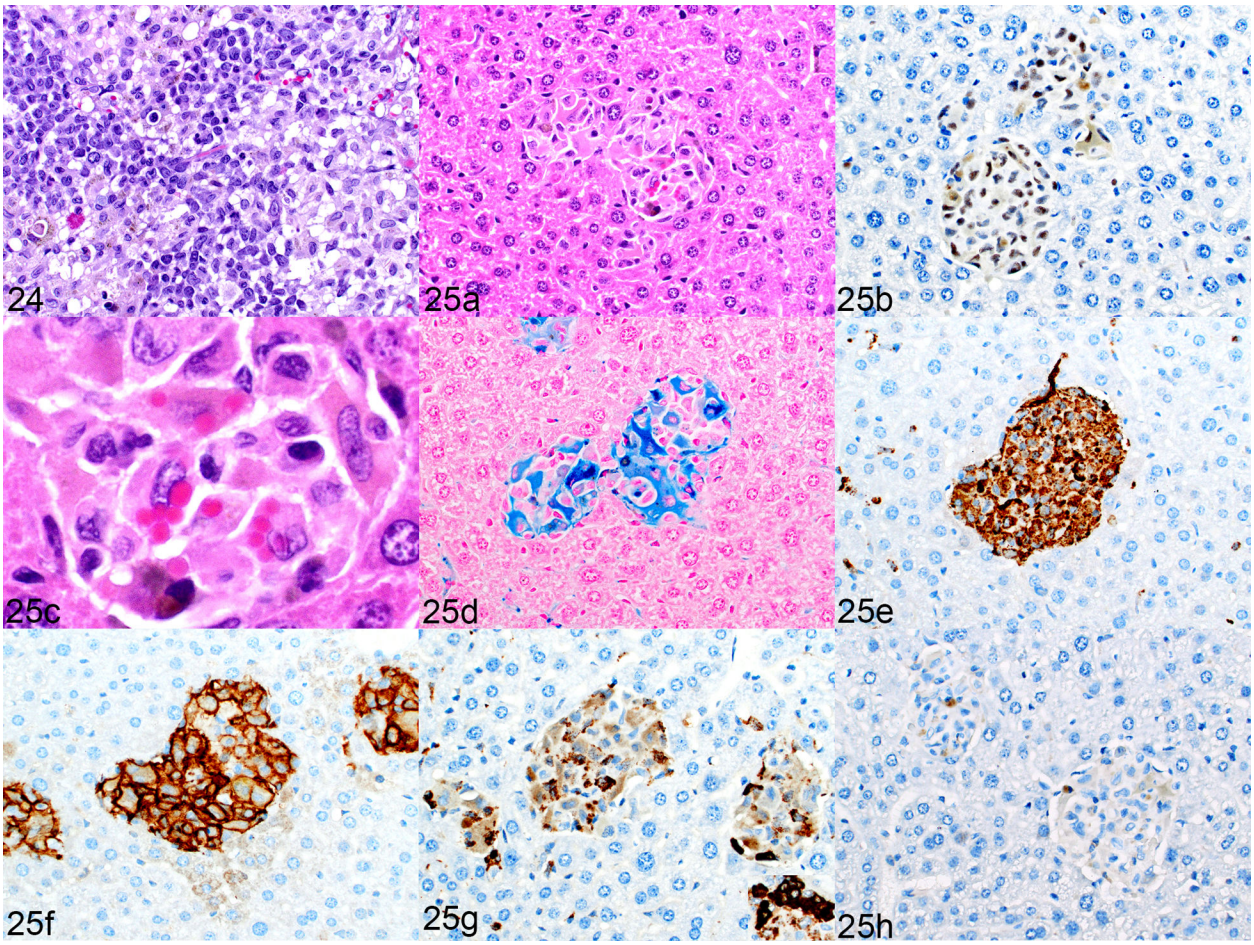

Figures 24 and 25.

NRG-SGM3 mice implanted with an acute myeloid leukemia (AML) patient-derived xenograft. **Figure 24**. Myelomonocytic human leukemia, bone marrow, mouse no. 21. HE. **Figure 25.** Macrophage proliferation, liver, mouse no. 21. (a, b, c) Cells are large, contain cytoplasmic pigment (a, HE), are immunolabeled for hNuMA1 (b). (c) Higher magnification of Figure 25a. Occasional erythrophagocytosis is present. (d–f) The cytoplasm labels positively for iron (d, Prussian blue), and the cells are immunolabeled for hCD68 (e) and hCD163 (f). (g) Only occasional cells are positive for myeloperoxidase (darkly immunolabeled cells are positive, weak immunolabeling is nonspecific). Inset: Leukemia cells in the kidney had a higher level of myeloperoxidase expression suggesting that this population in the liver is not the leukemia cells. (h)There is an absence of CD3 immunolabeling (small brown dots are iron pigment, not labeling of T cells), similar to the mouse with engrafted AEL in Figure 22h.

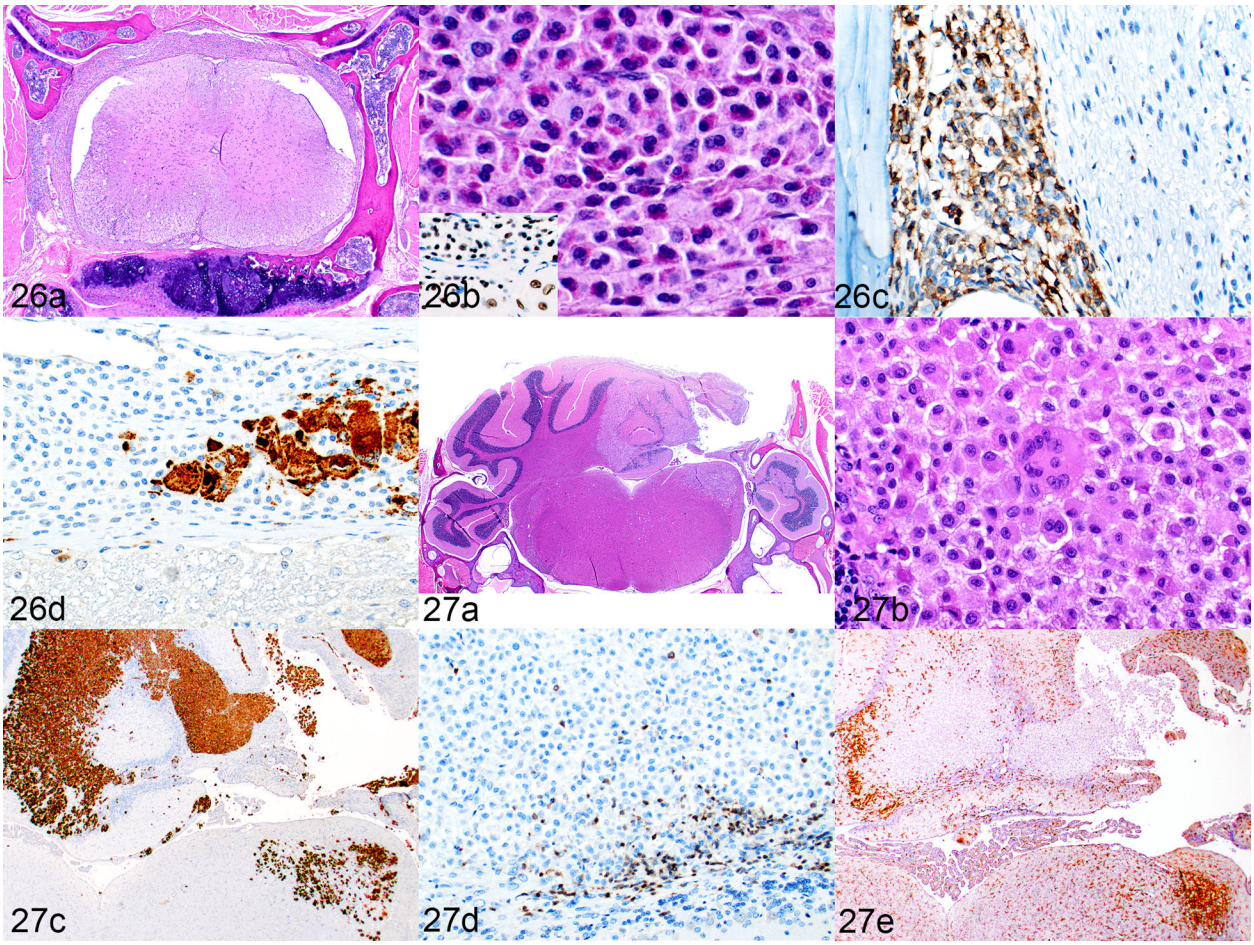

Figures 26 and 27.

Inflammatory cell infiltration of the CNS, humanized SGM-SGM3 mice. **Figure 26.** Spinal cord (mouse no. 2). (a) Vertebra and spinal cord cross-section. The meninges are thickened by mixed, patchy infiltrates of immune cells. HE. (b) One area shows prominent eosinophils. HE. Inset: immunolabeling for hNuMA1. (c) In other areas, the infiltrate is more lymphocytic, predominantly consisting of CD3-positive T cells. (d) Multiple foci of hCD68-positive macrophages are scattered in the meninges. **Figure 27.** Cerebellum, mouse no. 9. (a) Marked infiltration of macrophages in the right dorsal quadrant. HE. (b) The infiltrating cells are moderate to large in size, and there are occasional multinucleated giant cells. However, there is no cytoplasmic pigment as seen in cells in the spleen and liver. HE. (c) There is extensive infiltration of the cerebellum by hCD68-labeled cells. (d) Small numbers of CD3-positive T cells are present and only at the periphery of the lesion. (e) Reactive, proliferating cells that are immunolabeled for mouse F4/80- are present in the brain parenchyma bordering the macrophage infiltration.

Table 1.

Experimental Details of 24 Affected NSG-SGM3/NRG-SGM3 Mice

Mouse No.	Institution	Model	Sex	Age (weeks)	Implantation to Euthanasia (Weeks)	Clinical Signs
1	UC Davis	Humanized	F	29	25	Head tilt
2	UC Davis	Humanized	F	29	25	Hind limb paralysis
3	UC Davis	Humanized	F	32	28	Head tilt, lateral recumbency
4	UC Davis	Humanized	F	29	25	Ataxia, hunched posture, pallor, lethargy
5	UC Davis	Humanized	F	15	11	Pallor, lethargy, weight loss
6	UC Davis	Humanized	F	15	11	Hunched posture, pallor, weight loss
7	UC Davis	Humanized	F	15	11	Hunched posture, pallor, weight loss
8	UC Davis	Humanized	F	26	22	Head tilt, ataxia, weight loss
9	UC Davis	Humanized	F	32	28	Head tilt, ataxia
10	U Mich	Humanized	F	36	32	Pallor, lethargy, weight loss
11	U Mich	Humanized	F	38	34	Pallor, lethargy, weight loss
12	U Mich	Humanized	F	42	38	Pallor, lethargy, weight loss
13	MDA	Humanized	F	20	16	Failure to thrive
14	MDA	Humanized	F	20	16	Failure to thrive
15	St. Jude	Transduced hCD34+ HSCs	F	20	12	Hunched posture, pallor, weight loss, lethargy
16	St. Jude	Transduced hCD34+ HSCs	F	20	12	Hunched posture, pallor, weight loss, lethargy
17	St. Jude	Transduced hCD34+ HSCs	F	26	18	Hunched posture, lethargy
18	St. Jude	PDX, AEL #1	F	13	4	Pallor, weight loss
19	St. Jude	PDX, AEL #2	F	14	5	None reported
20	St. Jude	PDX, AEL #3	M	41	32	None reported
21[a]	St. Jude	PDX, AML #1	F	28	20	None reported
22[a]	St. Jude	PDX, AML #1	F	28	20	None reported
23[a]	St. Jude	PDX, AML #1	F	28	20	None reported
24[a]	St. Jude	PDX, AML #1	F	28	20	None reported

Abbreviations: UC Davis, University of California at Davis; U Mich, University of Michigan; F, female; M, male; HSCs, hematopoietic stem cells; PDX, patient derived xenograft; AEL, acute erythroid leukemia; AML, acute myeloid leukemia

[a]NRG-SGM3 strain

Table 2.

Clinical Characteristics of NSG Mice with Histiocytosis

Mouse No.	Model	Age (Weeks)	Time After Implantation (Weeks)	Presence of mild hemophagocytosis
25	Transduced hCD34+ HSCs	32	40	No
26	Transduced hCD34+ HSCs	32	40	Yes
27	PDX, B-ALL #1	20	10	No
28	PDX, B-ALL #2	N/K[a]	N/K	No
29	PDX, B-ALL #3	20	10	Yes
30	PDX, B-ALL #4	36	26	Yes

Abbreviations: HSCs, hematopoietic stem cells; PDX, patient derived xenograft; B-ALL, B-acute lymphoblastic leukemia

[a]Not known

Table 3.

Number of mice evaluated for each model and strain

Mouse Strain	Human Cells	Number of Mice Evaluated
NSG	Transduced hCD34+ HSCs	5
NSG	Leukemia B-ALL PDX, derived from 15 patients	18
NSG-SGM3	Naïve	3
NSG-SGM3	Humanized, hCD34+ HSCs	14
NSG-SGM3	Transduced hCD34+ HSCs	3
NSG-SGM3	Leukemia AEL PDX, derived from 3 patients	8
NRG-SGM3	Leukemia AML PDX, derived from 1 patient	16

Abbreviations: HSCs, hematopoietic stem cells; AEL, acute erythroid leukemia; PDX, patient derived xenograft; AML, acute myeloid leukemia

Table 4.

Immunohistochemistry methods for antibodies used in the study

Antigen	Species[a]	Dilution	Source, Catalog No.	Platform	Antigen Retrieval	Visualization
hNuMA1	H	1:75	Lifespan Biosciences, LS-B11047	Ventana[b]	HIER, CC2[c]	OmniMap[d]
CD117 /c-Kit	H/M	1:200	Dako Agilent, A4502	Ventana	HIER, CC1[e]	IVIEW[f]
MCT	H/M	1:6000	Abcam, ab151757	Ventana	HIER, CC2	OmniMap
hMBP	H	1:20	Bio-Rad, MCA5751	Ventana	HIER, CC2	OmniMap
mMBP	M	1:3000	Mayo, MT-14.7	Biocare[g]	EIER[h]	Bio poly[i]
hCD68	H	1:50	Dako Agilent, M0876	Ventana	HIER, CC1	IVIEW
hCD163	H	1:50	Cell Marque, MRQ-26	Ventana	HIER, CC1	IVIEW
F4/80	M	1:500	Invitrogen, MF48000	Biocare	HIER, TR[j]	Biotinyl[k]
hCD45	H	RTU[l]	Ventana, 760-2505	Ventana	HIER, CC1	OmniMap
CD3	H/M	1:1000	Santa Cruz, sc-1127	Ventana	HIER, CC1	OmniMap
PAX5	H/M	1:1000	Abcam, ab109443	Leica[m]	HIER, ER2[n]	BPRD[o]
hCD4	H	RTU	Leica, PA0427	Leica	HIER, ER2	BPRD
hCD8	H	RTU	Leica, PA0183	Leica	HIER, ER1[p]	BPRD
GFP	N/A	1:2000	CLONTECH, 632381	Ventana	HIER, CC2	Purple[q]
GATA1	H/M	1:4000	Abcam, ab131456	Ventana	HIER, CC1	OmniMap
MPO	H/M	1:1200	Dako, A0398	Ventana	HIER, CC1	OmniMap

Abbreviations: MCT, mast cell tryptase; MBP, major basic protein; GFP, green fluorescent protein; MPO, myeloperoxidase

[a] Species reactivity; H, human; M, murine; N/A, not applicable

[b] Ventana DISCOVERY ULTRA automated stainer, Ventana Medical Systems, Inc, Tucson, AZ

[c] Heat-induced epitope retrieval, Cell conditioning media 2, Ventana Medical Systems, Inc

[d] DISCOVERY OmniMap anti-rabbit HRP (760-4311), DISCOVERY ChromoMap DAB kit (760-159); Counterstain Hematoxylin II (Roche, Indianapolis, IN, 790-2208) and Blueing reagent (Roche, 760-2037)

[e] Heat-induced epitope retrieval, Cell conditioning media 1, Ventana Medical Systems, Inc

[f] IVIEW DAB Kit (760-091); Counterstain Hematoxylin II (Roche, Indianapolis, IN, 790-2208) and Blueing reagent (Roche, 760-2037)

[g] intelliPATH FLX, BioCare Medical, LLC, Pacheco, CA

[h] Enzyme-induced epitope retrieval with Proteinase K, DAKO S3020

[i] Rabbit anti-rat secondary antibody (Vector Labs, BA-4001), Rabbit-on-Rodent AP-Polymer (BioCare Medical, Concord, CA, RMR625H), and Fast Red chromogen kit (BioCare Medical, IPK5017G80); Counterstain hematoxylin (BioCare Medical, IPCS5006L)

[j] HIER with Decloaking Chamber NsGEN and Target Retrieval, pH 6

[k] Biotinylated rabbit anti-rat IgG, mouse absorbed secondary antibody (Vector Labs, BA-4001); Lab Vision streptavidin peroxidase (Thermo Scientific, TS-125-HR); DAB chromogen kit (Thermo Scientific, TA-125-QHDX); Counterstain hematoxylin (BioCare Medical, IPCS5006L)

[l] RTU, ready to use

[m] Leica BOND-MAX automated stainer, Leica Biosystems, Buffalo Grove, IL

[n] HIER with Bond Epitope Retrieval Solution 2 (ER2)

[o] Bond Polymer Refine Detection (DS9800); Counterstain Hematoxylin Refine Kit (Leica Biosystems, DS9800)

[p] HIER with Bond Epitope Retrieval Solution 1 (ER1)

[q] DISCOVERY OmniMap anti-rabbit HRP (760-4311), DISCOVERY ChromoMap Purple kit (760-229); Counterstain Hematoxylin II (Roche, Indianapolis, IN, 790-2208) and Blueing reagent (Roche, 760-2037)

Table 5.

CBC Values in NSG-SGM3 Mice. Representative examples for humanized mice, mice implanted with transduced hCD34+ cells and mice implanted with an AEL PDX, compared to typical values for naïve NSG-SGM3 mice.

	Naïve, Range[a]	Naïve, Mean	Humanized Mouse[b]	Transduced hCD34+ HSCs[c]	Engrafted AEL PDX[d]
HCT, %	32.4–37.5	33.9	8.3	7.0	19.5
RBC × 10^6/μL	6.5–7.79	7.2	1.25	1.12	3.47
HB, g/dL	10.2–13.1	11.6	2.2	3	5.7
MCV, fL	48.1–49.8	47.2	66.2	62.5	26.1
MCH, pg	15.7–16.8	16.2	17.6	26.8	16.4
MCHC, g/dL	31.5–34.9	34.3	26.5	42.9	29.2
RETIC, x1000/ μL	12.5–120.9	54.8	N/D[e]	126.3	123.5
RETIC %	0.16–1.86	0.8	N/D	11.28	3.56

Abbreviations: CBC, complete blood count; AEL, acute erythroid leukemia; PDX, patient derived xenograft; HSCs, hematopoietic stem cells; HCT, hematocrit; RBC, red blood cells; HB, hemoglobin; MCV, mean corpuscular volume; MCH, mean cell hemoglobin; MCHC, mean cell hemoglobin concentration; RETIC, reticulocyte

[a] CBC values for 3 naïve NSG-SGM3 mice, showing range and mean.

[b] Mouse no.12

[c] Mouse no.16

[d] Mouse no. 20

[e] N/D, not done

Vet Pathol. Author manuscript; available in PMC 2022 January 01.

Table 6.

Summary of Models and Histopathologic Features Present

Mouse Strain	Human Cells	Mast Cell Hyperplasia	Eosinophil Hyperplasia	Histiocytosis with or without hemophagocytosis	Secondary HLH/MAS-Like Disease	Secondary HLH/MAS-Like Disease with CNS Involvement
NSG	None[a]	-	-	-	-	-
NSG	Humanized (hCD34+ HSC)[b]	-	-	+, subset	-	-
NSG	Transduced hCD34+ HSC[c]	-	-	+, subset	-	-
NSG	Leukemia PDX[c]	-	-	+, subset	-	-
NSG-SGM3	None[c]	+, M[d]	-	-	-	-
NSG-SGM3	Humanized (hCD34+ HSC)[c]	+, M and H[e]	+, H	-	+, subset	+, subset
NSG-SGM3	Transduced hCD34+ HSC[c]	+, M and H	+, H	-	+, subset	-
NSG-SGM3 or NRG-SGM3	Leukemia PDX[c]	+, M and H	+, H	-	+, subset	-

Abbreviations: HLH/MAS, hemophagocytic lymphohistiocytosis/ macrophage activation syndrome; CNS, central nervous system; HSC, hematopoietic stem cell; PDX, patient derived xenograft

[a] Historical controls

[b] As reported in reference 39

[c] Described in current manuscript

[d] M, murine cells

[e] H, human cells